Learning Interaction Primitives for Biomechanical Prediction

by

Geoffrey M. Clark

A Dissertation Presented in Partial Fulfillment
of the Requirements for the Degree
Masters of Science

Approved July 2018 by the
Graduate Supervisory Committee:

Heni Ben Amor, Chair
Jennie Si
Visar Berisha

ARIZONA STATE UNIVERSITY

August 2018

ABSTRACT

This dissertation is focused on developing an algorithm to provide current state estimation and future state predictions for biomechanical human walking features. The goal is to develop a system which is capable of evaluating the current action a subject is taking while walking and then use this to predict the future states of biomechanical features.

This work focuses on the exploration and analysis of Interaction Primitives (Amor *et al.*, 2014) and their relevance to biomechanical prediction for human walking. Built on the framework of Probabilistic Movement Primitives, Interaction Primitives utilize an EKF SLAM algorithm to localize and map a distribution over the weights of a set of basis functions. The prediction properties of Bayesian Interaction Primitives were utilized to predict real-time foot forces from a 9 degrees of freedom IMUs mounted to a subjects tibias. This method shows that real-time human biomechanical features can be predicted and have a promising link to real-time controls applications.

To the love of my life

First, I want to truly thank my advisor Dr. Heni Ben Amor, who through his patience and encouragement has provided me to tools to become successful in research. Heni, you did not have to take me on as a masters student, especially since I was busy and sometimes slow to get results, but you did. You have been a constant champion of my research and a wonderful advisor, without your backing and fortitude I am sure I would not have completed this work. Thank you.

I would also like to acknowledge Dr. Jennie Si, who has supported me in my learning and the development of my knowledge of machine learning. I greatly appreciate the way in which you have made yourself available to me, especially when I have been seeking advice or needing answers. Your knowledge and guidance continues to be a boon to my success as a student.

I have received the help and support of a great number of people, especially, but not limited to, my colleagues Joe Campbell and Trevor Richardson who have offered their knowledge and code freely. I am indebted to you for always graciously answering my questions and helping me with my work.

I thank my family for their constant support and encouragement. Even when I cant properly describe what I am working on you smile and pretend it is interesting. Your financial support and empowerment are the reason I am here today. Thank you.

Lastly, but absolutely not least, my wife, Brittney, has been a source of steadfast and unconditional love during these years of schooling. Your Support, love, and devotion to me and our family means more to me than I can express with words. I will do my very best to make these hectic years worth it to us both.

I gratefully acknowledge the financial support I received from the School of Earth & Space Exploration.

TABLE OF CONTENTS

Page

LIST OF TABLES vi

LIST OF FIGURES vii

CHAPTER

1 INTRODUCTION 1

1.1 Introduction 1

1.2 Overview 3

2 BACKGROUND INFORMATION 6

2.1 Imitation Learning in Collaboration 6

2.2 Interaction with Probabilistic Movement Primitives 8

2.2.1 ProMPs for a Single DOF 9

2.2.2 ProMPs for Interaction 10

2.3 Phase Detection 13

2.4 Bayesian Interaction Primitives 14

2.5 Key Gait Biomechanics 16

3 SENSOR CONSTRUCTION AND PERFORMANCE 18

3.1 Force Sensitive Shoe Platform 18

3.2 IMU Platform 20

3.3 Hardware Setup 22

3.4 Software 24

4 LEARNING PRIMITIVES FOR HUMAN WALKING 25

4.1 Transitioning to Cyclical Interaction Primitives 29

4.1.1 Phase Projection 31

4.1.2 Basis Functions 36

5 EXPERIMENTS 44

CHAPTER Page

5.1 Data Collection 45
5.2 Data Analysis 47
5.2.1 Principal Component Analysis 47
5.3 Phase Projection Analysis 51
5.3.1 Projection Analysis 51
5.3.2 Phase Coherence 53
5.4 Basis Function Comparison 56
5.4.1 Reproduce Mean of Trajectories 57
5.4.2 Reproduce Distribution of Trajectories 59
5.5 Learning Level Ground Interactions 63
5.6 Learning Sloped Interactions 67
5.7 Learning Stair Climbing Interactions 72
6 CONCLUSION AND FUTURE WORK 76
6.1 Conclusion 76
6.2 Future Work 76
6.2.1 Human State Estimation and Biomechanical Prediction 77
6.2.2 Symbiotic Control Algorithms 80
REFERENCES 83

LIST OF TABLES

Table Page

5.1 Feature Coherence Evaluation 54

5.2 Trajectory Reproduction Error 58

5.3 Level Ground Walking Prediction Errors 63

5.4 Inclined Walking Prediction Errors 68

5.5 Stair Walking Prediction Errors 72

LIST OF FIGURES

Figure Page

1.1 Algorithmic Flow Diagram 5

3.1 Force Sensitive Shoe Platform 19

3.2 Shoe Platform Sensor Locations 20

3.3 IMU Platform 21

3.4 IMU Platform 21

3.5 IMU Mounting Constraints 23

4.1 ProMP First Step Prediction 28

4.2 Repeating Walking Cycle 28

4.3 Human Walking Gait Cycle 30

4.4 Tibia Limit Cycle 30

4.5 Phase Plane of Tibia at Different Speeds 32

4.6 Phase Plane of Tibia 33

4.7 Phase Mapping of Tibia Limit Cycle 34

4.8 2D Phase Surface Projection 35

4.9 3D Phase Surface Projection 35

4.10 Gaussian Basis Functions 36

4.11 Typical Trajectory 37

4.12 Gaussian Basis Function Weights for Trajectory 37

4.13 Trajectory Reproduction with Gaussian Basis Functions 38

4.14 Fourier Series Basis Function 39

4.15 Sines Approximation of Angular Position 40

4.16 Sines Approximation of Angular Velocity 40

4.17 von Mises Basis Functions 42

4.18 von Mises Approximation of Angular Position 42

Figure Page

4.19 von Mises Approximation of Angular Velocity 43
5.1 PCA Analysis on Walking Data 49
5.2 Variable Explanation of Variance by PCA 51
5.3 Phase Projection 2D 52
5.4 Phase Projection 3D 53
5.5 Tibia Angular Velocity in Phase 55
5.6 Heel Force in Phase 55
5.7 Toe Force in Phase 56
5.8 von Mises Approximation of Angular Position Distribution 60
5.9 von Mises Approximation of Angular Velocity Distribution 60
5.10 Sines Approximation of Angular Position Distribution 61
5.11 Sines Approximation of Angular Velocity Distribution 61
5.12 Sample Trajectories from the Angular Position Distribution 62
5.13 Sample Trajectories from the Angular Velocity Distribution 62
5.14 Foot Force Prediction on Level Ground Walking 64
5.15 Foot Force Prediction vs. Observations on Level Ground Walking 65
5.16 3D Foot Force Prediction 66
5.17 Foot Force Prediction on Inclines 69
5.18 Foot Force Prediction vs. Observations on Inclines 70
5.19 3D Foot Force Prediction for Inclines 71
5.20 Foot Force Prediction on Stairs 73
5.21 Foot Force Prediction vs. Observations on Stairs 74
5.22 3D Foot Force Prediction for Stairs 75
6.1 SpringActive inc. Odyssey Robotic Ankle 77

Chapter 1

INTRODUCTION

1.1 Introduction

Bipedal locomotion is a fundamental motor skill for humans. In urban environments adults walk about 6,500 steps per day and children usually double that. Yet for many, amputations are unavoidable. Diabetes (72%), infections (8%), and trauma (7%) are the leading causes of amputation. Furthermore, 90% of all amputations affect the lower leg. With approximately 185,000 new lower-limb amputations in the United States each year, novel prosthetic technology has the potential to restore human capabilities that have been previously lost. Enabling these technologies will improve millions of peoples' lives. Unfortunately, even advanced, powered prosthetics are far from this vision.

Most prosthetics controls implementations have focused on a tuned mechanical or impedance based, spring damper system to mimic the Achilles tendon of an able-bodied individual (Holgate *et al.*, 2009). These systems utilize controllers that output a desired actuator position based on IMU sensor data. The major limitations of these simple controllers are that the actuator position profile must be tuned for each amputee, they do not easily map to different gait patterns such as slopes or stairs, and once tuned the quality of the profile degrades as walking speed moves away from the speed at tuning. As a result, these limitations lead to unintended biomechanical and ergonomical ramifications on the human body. Actions which the controller deems correct can be applying unnecessary internal stresses to the human musculoskeletal system. This has been proven to lead to serious chronic secondary conditions such as

osteoarthritis (OA) (Morgenroth *et al.*, 2012).

While a myriad of factors contribute to the development of OA in amputees, the most notable cause is the repeated cyclical loading caused by walking with an asymmetrical gait (Royer and Koenig, 2005). Since amputees will often develop unique gait characteristics from others with similar pathological conditions (McNealy and A. Gard, 2008), each different condition presents unique challenges to tuning individual prosthetic devices for an amputee. The main reason these controllers are in such prevalent use is the fact that it is notoriously hard to anticipate the many possible biomechanical variables as well as the correct prosthetic response in every situation. To properly accommodate able-bodied movement while maintaining biomechanically sound actuation it is necessary to develop a transformative method for human-machine symbiosis which can predict, in real-time, biomechanical features across multiple walking gaits and conditions.

Leg prosthetics must possess the basic skills to interact with human movement in both known and unknown environments. Programming a controller with such high-level skills is a difficult task, as each individual has a different natural body movement that will produce different timing and gait motion. Imitation Learning, or learning from demonstrations, is ideal for this application as it allows for the complex relationships of the human walking system to be learned without generic patterns or controls. By learning the relationships between and being able to predict current and future biomechanical variable such as joint forces and moments a prosthetic device could steer the human robot interaction towards a biomechanically safe movement regime.

To this end, I introduce Predictive Biomechanics - a novel biomechanical feature prediction, such as internal force prediction, to create generalized predictions from observed data of a human subject. In contrast to traditional controls or system iden-

tification solutions, which focuses on creating generalized rigid solutions, Predictive Biomechanics seeks to create an adaptive model of human force interaction which can be used in countless locomotive situations while accurately predicting future states based on current actions. Built on the framework of Probabilistic Movement Primitives, Interaction Primitives utilize a novel method to localize and map a distribution over the weights of a set of basis functions. The goal of this project is to utilize the prediction properties of the Probabilistic Movement Primitives (Maeda *et al.*, 2014) to predict real-time foot forces from IMUs mounted to a subjects tibias during human walking motion. Being able to show that complex biomechanical human walking features are able to be predicted in real-time will show that Probabilistic Movement Primitives can also be used for prediction and control in prosthetic devices.

The outline of this Dissertation is as follows; Chapter two gives a brief description of the background and math that accompanies: Probabilistic Movement Primitives and the extension into interaction primitives along with key insights into human walking. Chapter three is an overview of the construction and performance of the sensors used in data collection and testing. Chapter four describes the tasks and algorithmic setup. Chapters five and six outline the experiments and denote important results obtained through the experimentation, respectively. Finally, Chapter seven expresses conclusions and notable future work.

1.2 Overview

The following overview covers the system flow of the finished algorithm. Illustrated in Figure 1.1 is the complete algorithm and setup including the steps for learning, testing and validation. In the following section each of these steps is explored and the details of how each section applies to the next is related. The following diagram is split up into two main portions, the learning stage where learning through demonstration

is done and the execution stage where testing and validation is accomplished.

The learning methods are comprised of two main tasks. The first task is to create the phase projection surface covered in Section 4.1.1. In order to create this surface a set of prerecorded data is used and cut up into a set of individual steps using the heel sensor as an indicator of heel strike. Each step demonstration contains all of the data from both IMUs and both shoes as a trajectory in time from the start of one step to the start of the next. These demonstrations are passed into the custom program which uses the biomechanical features within the data to generate the Phase Projection surface.

Second, the preprocessing task must generate the mean and covariance of of the demonstrations such that they can be used later on in the cyclical interaction primitives. Previously generated step demonstrations are put through the Phase Projection method in order to put the data in the phase domain instead of in time. Generated step demonstrations in phase are then used as per Section 2.2.2 to create the mean and covariance of the trajectories using von Mines Basis Functions described in Section 4.1.2.

The execution stage focuses on the live testing and validation of the data. As such the testing stage takes live data observations as input data and first using the Phase Projection surface, developed in the Learning step, generates the current phase estimation. This phase estimation and the original observation and input into the Cyclical Interaction Primitives in order to find the current foot force prediction.

Foot force prediction is then sent to the validation stage where it is compared against live observations of the foot force in two ways. First it is plotted directly against the actual foot force to get an idea of how the prediction compares. Second the mean squared error(MSE) and mean absolute percent error(MAPE) are calculated to find the amount of difference between the predicted and actual forces.

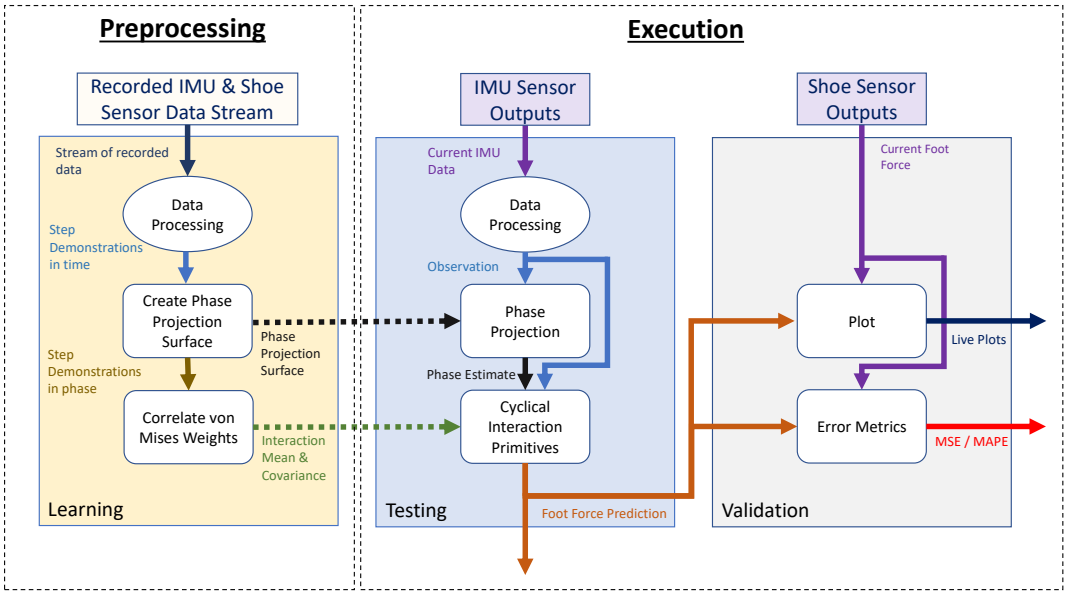

Figure 1.1: Diagram illustrating the three main portions of the designed algorithm and the data transfer through them.

Chapter 2

BACKGROUND INFORMATION

This chapter gives an introduction to previous and relevant work in literature related to Imitation Learning, Interaction Primitives, phase detection, and Bayesian Interaction Primitives. These concepts form the conceptual backbone for why Interaction Primitives are used in this work and are imperative to gain an understanding of this Dissertation. The subsequent sections focus on the background and general information regarding classical Imitation Learning and their accompanying details.

2.1 Imitation Learning in Collaboration

Imitation Learning is a machine learning process that aims to mimic human behavior in a specific task. This idea, often called programming by example or learning from demonstration, is one in which an agent is trained to implement a behavior from demonstrations by learning relationships between observations and actions. Despite the fact that this method has been around for many years it has recently gained traction due to advances in computation and sensing. Systems are often too complex to program by hand and accurately depict interactions between robots and the environment (Schaal, 1999). Therefore, Imitation Learning is used because it allows for these complex tasks to be learned from a minimal number of expert demonstrations of the given task.

Aforementioned advances in computation and sensing has allowed Imitation Learning to expand considerably across many fields of research including: robotics, computer science, biology, and neuro-science, due to its prevalence and effectiveness in human and non-human mammals (Rao, 2005). Movement or locomotion by imitation

is a fundamental behavior in humans. We employ this ability nearly every day and are able to continuously able to both learn new tasks and modify old tasks based on demonstrations by ourselves and others. In fact, human infants can imitate body movements of others nearly from birth (Meltzoff and Moore, 1997). This type of learning is important because it limits the space in which learning is done. For example, a friend performs an action for you to mimic, even if you are not able to perfectly perform the action on the first try; the action simply being performed gives situational and biomechanical insight into how the action is performed such that it can be perfected during the next try.

While this method is important for biological systems it is equally as important for robotic systems. When a robotic systems needs to explore or modify actions in different environments to find optimal solutions to tasks, there is an exponential increase in the number of actions available to take in every state. Hence, the system becomes more and more complex causing the number of degrees of freedom or control inputs to increase. This means it is computationally implausible to search the entire space to determine good from bad actions, let alone for an optimal solution. In these cases, Imitation Learning is widely used to provide a more concise state-action space within which learning can be achieved (Hussein *et al.*, 2017). However, Imitation Learning has recently been extended from pure movement imitation to physical interaction by Lee *et al.* (2010) and then later to true human robot interaction (HRI) under the concept of Interaction Primitives (Amor *et al.*, 2014), (Maeda *et al.*, 2014); which allow robots to learn and execute collaborative tasks with a human or non-human partner.

2.2 Interaction with Probabilistic Movement Primitives

This section discusses the formulation of Probabilistic Movement Primitives (ProMPs) by showing how a single task can be warped into a low dimensional space of weights then decoupled from time with a phase variable. By then adding multiple demonstrations of the task a correlation can be built which describes the relationship between observations for a single degrees of freedom (DOF) as well as corresponding observations across all other DOF. An understanding of this description is fundamental for the following sections.

Interaction with ProMPs (Maeda *et al.*, 2014) is a formulation of Interaction Primitives which creates an interaction method that is able to recognize an observed action to then generate an appropriate movement primitive for the robot actor. This leveraging of Imitation Learning within a probabilistic framework is done by modeling the interaction probabilistically as a distribution of observations using ProMPs as described in (Paraschos *et al.*, 2013). Such a distribution can be obtained by observing the interaction a number of times and recording the trajectories in all degrees of freedom and time. These trajectories can then be used to create a prior model of the interaction space where the trajectories are decomposed into a set of weights of basis functions. In the event that a new partial observation is obtained the model is able to recognize the intention of the observed agent and will use the correlation between the observations and the actions from the demonstrations to generate an action to control the robot.

The following section Section 2.2.1 illustrates the concept of ProMPs with a single DOF. Then, methodology and main characteristics of using the ProMPs in Interaction Primitives will follow in Section 2.2.2.

2.2.1 ProMPs for a Single DOF

For the following derivations a DOF will refer to any robot or human sensor or joint with position q and velocity $\dot{q}$. Since this is a single DOF, we denote the state vector trajectory $y(t) = [q(t)\ \dot{q}(t)]^T$ as the sequence $\tau = \{y(t)\}_{t=0,\dots,T}$. By adopting linear regression with n Gaussian basis functions ψ, the state vector can be characterized with an n-dimensional column vector of weights w as

$$y(t) = \begin{bmatrix} q(t) \\ \dot{q}(t) \end{bmatrix} = \begin{bmatrix} \psi(t) \\ \dot{\psi}(t) \end{bmatrix} w + \epsilon_y.$$

In this case $\Psi = \begin{bmatrix} \psi(t) \\ \dot{\psi}(t) \end{bmatrix}$ is a $2xn$ dimensional time-dependent matrix of basis functions. The assumption being made here is that the noise variable $\epsilon_y \sim \mathcal{N}(0, \Sigma_y)$ is zero mean $i.i.d$ Gaussian noise. With this noise assumed the probability of observing the entire trajectory can be computed with

$$p(\tau|\omega) = \prod_{0}^{T} \sim (y(t)|\Psi_t\omega, \Sigma_y).$$

ProMPs are similar to Dynamic Movement Primitives in the way in which they are decoupled from time. For instance, instead of the speed of execution being linked directly to a rate in time, the speed of the original trajectory is decoupled from time using a phase variable $z(t)$. The phase variable is a direct replacement for time in the equations in order to control the location of the basis functions with $\psi(z(t))$. For this reason, the phase variable is directly substituted for time with $z(t) = t$ such that $\psi(t) = \psi(z(t))$. Keep in mind that $z(t)$ can be any monotonically increasing function (Paraschos *et al.*, 2013).

All of the trajectories in time are now represented by a low-dimensional space of basis function weights w in phase. This is done to reduce the complexity of the

problem since n number of basis functions used is usually much smaller than the number of time steps. In order to obtain an accurate representation of the space multiple demonstrations are required. Therefore, trajectory variations within the demonstrations are characterized by defining the distribution over the weights $p(\omega|\theta)$, where θ is the learning constant. Due to this, the probability of observing the whole trajectory becomes

$$p(\tau|\theta) = \int p(\tau|\omega)p(\omega|\theta)d\omega.$$

Hence, θ captures the correlation both between the individual weights within each trajectory, and between each DOF from trajectory to trajectory.

2.2.2 ProMPs for Interaction

Now we will discuss the intricacies of moving from ProMPs to a full state linear estimator of the controlled agent. The full state linear estimator utilizes a Kalman filter to recursively apply Gaussian conditioning to a matrix of basis weights. Estimations use the correlations across all DOF and an engineered measurement noise model. This type of stochastic filtering provides and optimal estimation of the controlled agent state based on the observed agent state and state estimation.

One key aspect of ProMPs necessary for the realization of Interaction Primitives is the use of the parameter θ. This parameter is extended to the expression of the correlation between all DOFs of multiple agents directly together using the correlation of their trajectories. The big assumption made in this work is that the distribution of trajectories of all DOFs including those of different agents is normal. Therefore $p(\omega|\theta) = \mathcal{N}(\omega|\mu_\omega, \Sigma_\omega)$, redefines the vector of weights ω to represent all DOF of all agents. Following the work made by Heni Ben Amor in Amor *et al.* (2014), the human agent will be referred to as the observed agent and the robotic system will be

referred to as the controlled agent. For a pure human robot interaction system these descriptions will hold, but this work can be extended to any interacting agent. Thus, the observed and controlled agents are not strictly required to be a human-robot pair.

In order to tie this formulation into Interaction Primitives, first a row vector of all DOF weights is constructed by concatenating the weights of the observed agent P followed by the weights of the controlled agent Q

$$\overline{\omega}_d = \left\{ \left[\omega_1^T, ...\omega_p^T, ...\omega_P^T\right], \left[\omega_1^T, ...\omega_q^T, ...\omega_Q^T\right] \right\}.$$

Where $\overline{\omega}_d$ is the full weight vector corresponding to the d-th demonstration, ω_p^T is the n-dimensional column vector of weights of the p-th DOF of the observed agent, and ω_q^T is the n-dimensional column vector of weights of the q-th DOF of the controlled agent. At this point, the mean (μ_ω) and covariance (Σ_ω) are computed by layering the weights from each demonstration as below where D is the number of demonstrations.

$$\mu_\omega = mean\left(\left[\omega_1, ...\omega_d, ...\omega_D\right]^T\right)$$
$$\Sigma_\omega = Cov\left(\left[\omega_1, ...\omega_d, ...\omega_D\right]^T\right)$$

Since the assumption was made that the distribution of trajectories of all DOF across the demonstrations is normal, Gaussian conditioning can be applied live as each new observation is collected by applying a Kalman filter in the form

$$K = \left(\Sigma_\omega^- * H_{z(t)}^T\right) * \left(\left(\left(H_{z(t)} * \Sigma_\omega^-\right) * H_{z(t)}^T\right) + \Sigma_y^*\right)^{-1}$$
$$\mu_\omega^+ = \mu_\omega^- + \left(K * \left(y^*(t) - H_{z(t)} * \mu_\omega^-\right)\right)$$
$$\Sigma_\omega^+ = \left(I - \left(K * H_{z(t)}\right)\right) * \Sigma_\omega^-.$$

The first equation is the Kalman gain equation where K is the Kalman gain matrix which controls the filters use of the current state estimate. The next two equations

generate a prediction for the state estimate and error covariance. In these equations the + and - symbols denote the predicted and previous states respectively. Finally, y_t^* denotes the observation at time-step t, Σ_y^* is the measurement noise, and δ is the current phase, independent of time. It is important to note here that in order to get an accurate prediction from the Kalman filter an accurate estimation of the phase state is required. Phase state estimation does not come from the Kalman filter, but from an outside algorithm which can produce phase estimation in real-time, this will be described more in Section 2.3. The observation matrix (H_δ) is a block diagonal matrix with each diagonal entry corresponding to each DOF of the observed agent as $2xn$ basis $\begin{bmatrix} \Phi_\delta^T \\ \dot{\Phi}_\delta^T \end{bmatrix}$.

$$H_\delta = \begin{bmatrix} \Phi_\delta^T & \dots & 0 \\ \vdots & \ddots & \vdots \\ 0 & \dots & \Phi_\delta^T \end{bmatrix}$$

The observation matrix includes the DOFs of both the observed and controlled agents, but in an interaction setting the goal is to use only the observed agent during the Gaussian conditioning stage. To orchestrate this setup and to maintain consistency with the previous definition of $\overline{\omega}_d$, where the entries are concatenated such that the observed agent comes before the controlled agent, the observation matrix is partitioned off into sections and the controlled agent weights are set to zero.

$$H_\delta = \left[\begin{array}{cc|cc} \left(\Phi_\delta^{To}\right)_{1,1} & 0 & 0 & 0 \\ 0 & \left(\Phi_\delta^T\right)_{(P,P)} & 0 & 0 \\ \hline 0 & 0 & 0^c_{(1,1)} & 0 \\ 0 & 0 & 0 & 0^c_{(Q,Q)} \end{array}\right]$$

Where the superscripts o and c denote the observed and controlled agents, respectively, and each 0 entry is on size $2xn$ dimensions to maintain consistency across the

matrix dimensions. In general, only a partial combination of observations is able to provide an optimal estimate since the Gaussian conditioning in the Kalman filter is a full state estimator.

2.3 Phase Detection

A main problem with Interaction Primitives using ProMPs is that an external algorithm is required to generate an estimation of the phase. The requirement is due in part to the tendency of demonstrations to be warped in time compared to one another. Human demonstrations, specifically, can be slower or faster than one another or even change locally. Any warping of this type must be corrected or time-aligned in order to achieve a valid state estimation. In most cases algorithms such as this time warping function below uses local optimization of the time warping function with

$$t_{\omega}^{j+1} = v_0^j + g(v^j)t_{\omega}^j.$$

Where t_{ω}^j represents a vector containing a raw time series of demonstration $y_{\omega}$with or without warping, at the j-th iteration of the optimization. In this case g is treated as a smooth, linear Gaussian basis model $v^j = \left[v_1^j, ..., v_B^j\right]$ with B weights, as optimization model. Also included is the time shift value v_0^j which is used when the reference trajectory and the trajectory to time-align are indistinguishable but start at different times. The basis weights are optimized using gradient descent with the objecting of decreasing the absolute cumulative error between the two trajectories.

$$v = argmin \sum_{k=0}^{K} |y_r(t_r(k)) - y_{\omega}(v_0^j + g(v^j)t_{\omega}^j)|$$

This method is slightly from the traditional Dynamic Time Warping (DTW) function seen in (Sakoe and Chiba, 1978). This local method which utilizes the smoothing function g gets around the traditional problems of DTW which include jumping the indexes and difficulty of tuning a slope constraint to help with smoothing. Additionally, the smoothing function acts to preserve the overall shape of the trajectory while shifting it into correct local alignment.

2.4 Bayesian Interaction Primitives

Bayesian Interaction Primitives (BIP) in Campbell and Amor (2017) extend the idea of Simultaneous Localization and Mapping (SLAM) into Interaction Primitives such that phase estimation and Bayesian inference are performed in the same step. Phase estimation is required when there is only a partial observation of the trajectory y^* and it is desired to obtain the controlled trajectory through Bayesian inference. The approach here is to view the goal of attaining a phase estimation as a localization problem instead of one of time alignment. Using an Extended Kalman Filter (EKF) localization, a map of N landmarks is used to find the pose s_t with respect to the landmarks. This phase variable $s_t = \delta_t$ is the robot state in the map of possible trajectories and shows where the robot is relative to the demonstrations. With this out of the way the demonstration weights, μ_ω and Σ_ω, can be represented by the map. To finish the implementation of SLAM in Interaction Primitives, the basis weights of the robot state replace the landmarks on the map such that, $s_t = \left[\begin{smallmatrix}\delta_t \\ \dot{\delta}_t\end{smallmatrix}\right] \in \mathbb{R}^{(D_o+D_c)B+2*1}$. Each basis weight of a basis function represents a single landmark. The relevant EKF SLAM equations are:

$$s_t = \begin{bmatrix} \delta_t \\ \dot{\delta}_t \\ \omega^T \end{bmatrix}$$

$$p(s_t|z_{1:t}) = \mathcal{N}(s_t|\mu_t, \Sigma_t)$$

$$\mu_0 = \begin{bmatrix} 0 \\ \beta \\ \mu_\omega^T \end{bmatrix}$$

$$\Sigma_0 = \begin{bmatrix} \Sigma_{\delta,\delta} & \Sigma_{\delta,\Sigma_\omega} \\ \Sigma_{\Sigma_\omega,\delta} & \Sigma_{\omega,\omega} \end{bmatrix}.$$

Where $\mu_t \in \mathbb{R}^{(D_0+D_c)B+2*1}, \Sigma_t \in \mathbb{R}^{(D_0+D_c)B+2*(D_0+D_c)B+2}$,$\beta$ is the phase velocity in the demonstrations, $z_{1:t} = y^*_{1:t}$ and $\Sigma_{\omega,\omega} = \Sigma_\omega$. This forms the constant velocity model,

$$\mu_t = \mu_{t-1} + \underbrace{\begin{bmatrix} 1 & 0 \\ \Delta t & 1 \\ \vdots & \vdots \\ 0 & 0 \end{bmatrix}}_{F} \begin{bmatrix} 1 \\ 1 \end{bmatrix} + \mathcal{N}(0, F^T \underbrace{\begin{bmatrix} \sigma_{\delta,\delta} & \sigma_{\delta,\dot{\delta}} \\ \sigma_{\dot{\delta},\delta} & \sigma_{\dot{\delta},\dot{\delta}} \end{bmatrix}}_{Q_t} F)$$

$$G_t = \begin{bmatrix} 0 \\ 0 \end{bmatrix}.$$

The measurement model remains the same as in traditional Interaction Primitives.

$$z_t = \underbrace{\begin{bmatrix} \Phi_\delta^T \omega_1 \\ \Phi_\delta^T \omega_2 \\ \vdots \\ \Phi_\delta^T \omega_{D_c} \end{bmatrix}}_{h(\mu_t)} + \mathcal{N}(0, \underbrace{\begin{bmatrix} \sigma_1 & 0 & \dots & 0 \\ 0 & \sigma_2 & \dots & 0 \\ \vdots & \vdots & \ddots & \vdots \\ 0 & 0 & 0 & \sigma_{D_c} \end{bmatrix}}_{R_t})$$

The main change is that the calculation of the Jacobian must now take into account the two new variables: phase and phase velocity. This is done by

$$H_t = \frac{\partial h(\mu_t)}{\partial x_t} = \begin{bmatrix} \frac{\partial \Phi_\delta^T \omega_1}{\partial \delta} & \frac{\partial \Phi_\delta^T \omega_1}{\partial \dot{\delta}} & \frac{\partial \Phi_\delta^T \omega_1}{\partial \omega_1} & \dots & \frac{\partial \Phi_\delta^T \omega_1}{\partial \omega_{D_c}} \\ \vdots & \vdots & \vdots & \ddots & \vdots \\ \frac{\partial \Phi_\delta^T \omega_{D_c}}{\partial \delta} & \frac{\partial \Phi_\delta^T \omega_{D_c}}{\partial \dot{\delta}} & \frac{\partial \Phi_\delta^T \omega_{D_c}}{\partial \omega_1} & \dots & \frac{\partial \Phi_\delta^T \omega_{D_c}}{\partial \omega_{D_c}} \end{bmatrix}.$$

By zeroing out the phase velocity and substituting in the basis function weights you get,

$$H_t = \frac{\partial h(\mu_t)}{\partial x_t} = \begin{bmatrix} \frac{\partial \Phi_\delta^T \omega_1}{\partial \delta} & 0 & \Phi_\delta^T & \dots & 0 \\ \vdots & \vdots & \vdots & \ddots & \vdots \\ \frac{\partial \Phi_\delta^T \omega_{D_c}}{\partial \delta} & 0 & 0 & \dots & \Phi_\delta^T \end{bmatrix}.$$

2.5 Key Gait Biomechanics

In persons with Trans-Tibial Amputations (TTA) it is common to find significant strength discrepancies between the legs due to the natural limb being significantly stronger than the prosthetic limb (Lloyd *et al.*, 2010). Noted strength difference can appear as different symptoms in different individuals but is usually characterized by an asymmetrical weight distribution with the center of mass shifter underneath the normal limb (Sanderson and Martin, 1997). A natural center of mass while walking is

necessary for efficient and healthy walking. If the center of mass shifts in an unnatural way towards one leg, that leg is forced to take on more weight and this leads to diminished gait efficiency and joint degradation (Agrawal *et al.*, 2013). Within TTA, asymmetrical gait is the leading cause of secondary conditions such as osteoarthritis.

Other secondary conditions associated with TTA are: lowered walking speed, reduction in the power generated during stance phase, increased medial loading in natural knee during loading, reduced medial/lateral ground reaction forces, and increased metabolic cost of normal activities such as walking, standing, and running (Svoboda *et al.*, 2012), (Winter and Sienko, 1988), (Mattes *et al.*, 2000). During normal gait function the knee extensors and plantar flexors are the dominant cause of forward motion. In persons with Trans-Tibial amputations it has been found that with the lack of these two functions, increases in hamstring function accounted for the difference by increasing power at the hip.

Finally, the last big difference in walking with a Trans-Tibial amputation is a decrease in step size (Farrokhi *et al.*, 2016). Generally speaking, the main reasoning behind this decrease is two fold. First, trans-tibial amputees are not able to generate the same push-off force and therefore take smaller steps. Second, a reduction in step length help to provide needed stability. Since step length is caused by these two functions it is not able to be addressed by modern treatment options.

Chapter 3

SENSOR CONSTRUCTION AND PERFORMANCE

A general purpose sensor network consisting of multiple IMUs and two force sensitive shoes were pertinent for the tasks. After reaching out to a few companies about each device type, it was decided that the optimal solution was to build customized platforms for each device. Of the shoe platforms commercially available all of them were deemed to be both too expensive and too unwieldy to be effective in the kind of testing desired. Likewise, off the shelf blue-tooth enabled IMUs were simply not powerful enough for this application. The desired requirements are: minimum 100Hz data rate, low latency pipeline (less than 5ms), low cost, and high accuracy with minimal noise. In light of the requirements noted above, it was necessitated that solutions for both shoe and IMU platforms would need to be custom built. Details regarding the end devices are as follows.

3.1 Force Sensitive Shoe Platform

The shoe platform is a custom force sensing device that uses four amplified barometric pressure sensors embedded in the shoe. With this custom platform, measurements can be gathered for human ground reaction forces in a single dimension at four individual points on the foot. In this case, force sensor locations are across the heel, toe, inner metatarsal, and outer metatarsal; Figure 3.2 below illustrates the sensor locations in greater detail. These four sensors locations allow a wide variety of feedback from a human user which includes, but is not limited to, heel strike detection, lateral or medial weight shift, and forward of backward weight shift. Having this combination of sensors allows for the calculation of center of force on the foot

and center of mass of a human assuming the subject stays relatively non-dynamic. In addition to custom placement, these particular pressure sensors are temperature compensated, absolute pressure sensors with 12bits precision and a 0.5ms response delay. Due to the high precision, high accuracy, and very fast response time, these sensors are perfect for collection data on dynamic human motion. The basis for all device communication is the Arduino platform that utilize the Adafruit Pro Trinket as the main microprocessor board. Platform communication with a PC is handled by a serial blue-tooth device, running at 115200baud.

Figure 3.1: Force Sensitive Shoe Platform

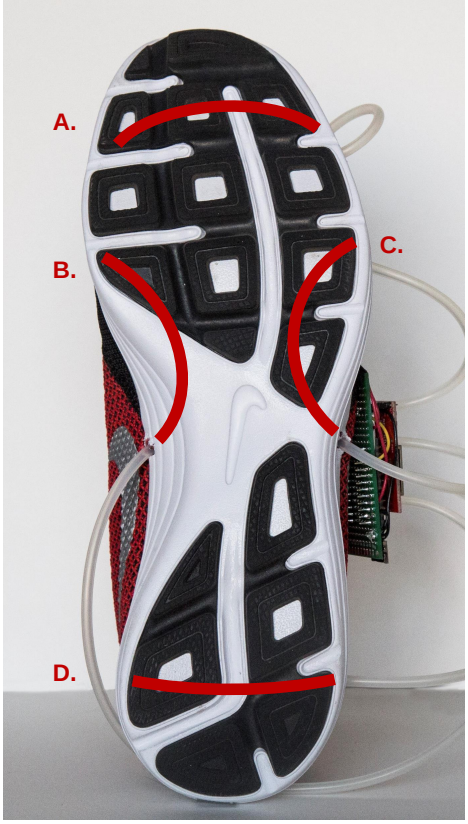

Figure 3.2: Shoe platform sensor locations: A. Toe sensor, B. Inner Metatarsal sensor, C. Outer Metatarsal sensor, D. Heel sensor.

3.2 IMU Platform

The IMU sensor uses the Arduino platform as the base of all device communication, for these units utilize the Adafruit Pro Trinket as the main microprocessor board, which takes 5V for an accompanying power board, also from Adafruit. The platform communication with a PC is handled by a serial blue-tooth device, running at 115200baud. Inertial sensing is handled by a BNO055 9-axis absolute position sensor and transmits requested data to the microprocessor via I2C communication standard. This device was chosen due to its high accuracy, high frequency, and unique features. As well as meeting the other requirements this sensor contains and on board

16-bit processor which does real-time absolute position calculations. This enables the sensor to send raw 3-DOF data for linear acceleration, angular velocity, and magnetic readings; as well as calculated linear position, angular position, and quaternion data. All data is collected with 16 bits of precision and the position and orientation of the coordinates can be seen in Figure 3.4 below.

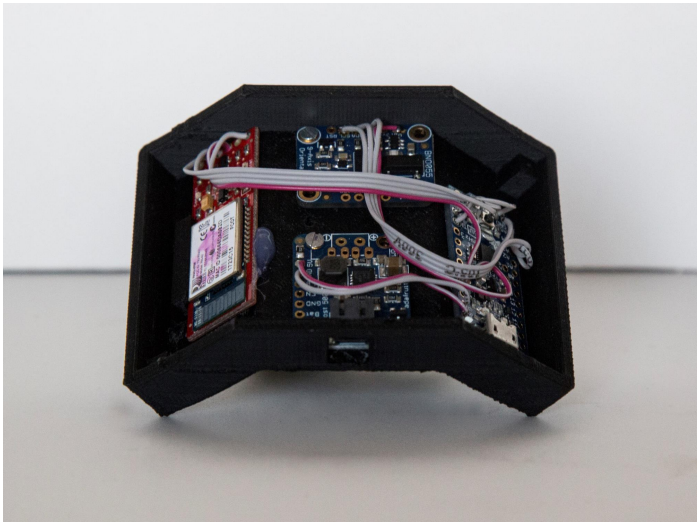

Figure 3.3: IMU Platform

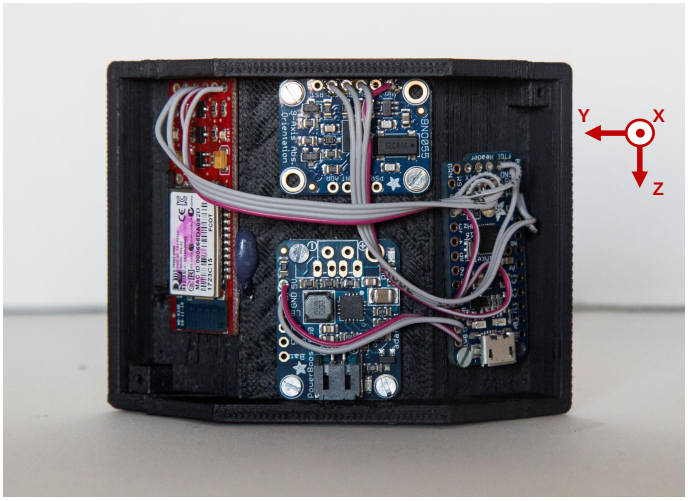

Figure 3.4: IMU Platform Front

3.3 Hardware Setup

Due to the nature of Interaction Primitives and the statistical methods that form them, this method is highly impaired by changes in the sensor mean, both within and between individuals tests. Due to the dynamic nature of human locomotion if a sensor slips or changes positing this will act to shift the observed sensor mean and therefore cause aberrant behavior in the algorithm. In the interest of minimizing this type of error it is imperative to mount the devices to the human subject in an easy and repeatable way. To this end the sensors, hardware, and mounting process were all engineered to maximize data integrity and to facilitate accurate and consistent data.

The IMU hardware shell was designed with a substantial concavity in order to better fit against the curvature of human limb, which enables the sensor to have a sound connection to the body and will therefore collect cleaner data. A flat sensor would have a tendency to want to tilt or shift against a curved human surface and would cause abnormal behavior in the sensor data. A simple Velcro strap was connected to the sensor body and will fit a wide variety of limb sizes. Additionally, it was found that the IMU sensor had a tendency to slip down the limb therefore a foam rubber sheet was adhered to the back of the sensor shell to create a better connection. All of the decisions made in the design of the shell greatly reduce the difficulty of mounting the device to a limb accurately. To insure sensor repeatability a single measurement is used to position the bottom of the sensor shell proximal to the subjects ankle joint. Lastly, the sensor is adjusted by eye while the subject is in a normal standing position to be even with the frontal plane. This setup ensures valid data during runtime.

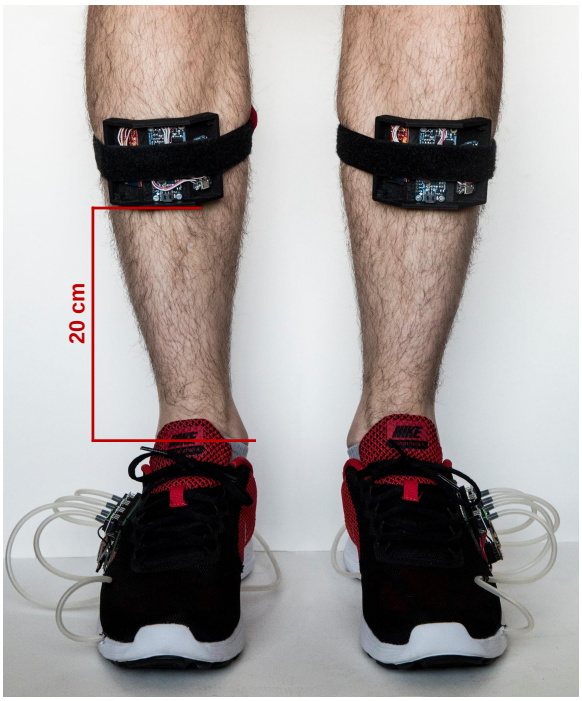

Figure 3.5: Mounting constraints for all units

Data integrity for the shoe sensors is a little trickier to maintain. Like the IMU sensors both mounting and hardware constraints impact the consistency of the data between tests. The barometric absolute pressure sensors are compensated to the ambient pressure, therefore as weather patterns or altitude change the sensors will not drift due to the environment. Instead, the drift was found during early trials to come from two sources, the placement of the foot within the shoes, and the method in which the shoe is laced up. In order to compensate for the first source of situational bias a hard insole was placed within the shoe which acts as a filter to transmit the forces from the foot to the sensors, while mitigating bias noise caused by foot placement. The second source of situational noise is more difficult in order to mitigate the bias noise caused by lacing it was imperative to develop a system which is repeatable and accurate. When viewing the data is it noted that the inner and outer metatarsal sensors are most affected by the lacing. This is because both the heel and toe sensors

are further away from the laces. Consequently, a process was put in place by which the the data is viewed in real-time while the foot is off the ground and being laced. The laces are then tightened until the foot in comfortably snug while minimal force is being exerted on the sensors by the lacing process. This ensures that pressure sensors are not pre-loaded and will give accurate force measurements.

3.4 Software

Robot Operating System (ROS) is a flexible software framework that was built to enable robotics software development. ROS provides a collection of tools and libraries with the purpose of simplifying the task of developing complex and robust robot behavior. This software framework provides features such as: libraries, visualization, messaging, package management, and hardware abstraction. In a practical sense ROS can best be described as a network of ROS nodes each running independently. Nodes can listen to or publish messages to specific topics which is how nodes communicate with one another.

The data pipeline for all sensors was built to utilize ROS because of the, ease of use, flexibility and robustness. Furthermore, the data pipeline through ROS has low latency, less than one millisecond, and a vast open-source community exist which makes development a breeze. A node is set up for each individual device, a low-level driver is written for each device type and the node interfaces with the driver to read serial data from the devices and then publish the data to the associated topic. This methodology provides a robot hardware abstraction layer such that real-time data can be maintained independent of hardware changes. In addition, the nodes are separate from one another if a single device fails or runs out of battery, the entire system does not fail. Figure 1.1 illustrates the entire data pipeline from device data to the main algorithm.

Chapter 4

LEARNING PRIMITIVES FOR HUMAN WALKING

Estimating biomechanical features from bipedal walking is a difficult problem for a number of reasons. Fist, the human body contains 244 DOF which makes for a very high dimensionality problem. In fact this only includes DOF of the positions of joints and does not include any biomechanical features such as internal or external stresses on the body. Optimal control theory is well suited to solving the generic problem and has been done successfully by: Lin *et al.* (2018), Ackermann and Van den Bogert (2010), Meyer *et al.* (2016), and Anderson and Pandy (2001). These types of solutions utilize control theory, traditional filtering methods, and system identification which are all well known and effective solutions in general, but cannot be tailored well to an individual. Other methods derived from pure mathematical models (Collins and Kuo, 2010), biomechanical observation (van Dijk and Van der Kooij, 2014), and even investigating through using humanoid robots to test methods (Ijspeert, 2014). Since each member of the population has a different body size and shape, relationships among joints while walking will likewise differ greatly. While there is research being done on the subject there is not a precise understanding of how these relationships change with differences such as: gender, weight, and height. This knowledge gap, means that the traditional model based design or model predictive control solutions are not going to be effective. Currently the only effective solutions proposed have involved manually tuning devices ether by an expert in the field, or through human-in-the-loop optimization such as in (Zhang *et al.*, 2017).

The question is how to get to an effective model. Statistician George Box said "Just as the ability to devise simple but evocative models is the signature of the

great scientist so over-elaboration and over-parameterization is often the mark of mediocrity." Or in layman's terms, simple effective models that can be dealt with and explored will always be more effective that those which are too complex to treat with effectively. Under this advice, I propose using a data driven approach that can effectively learn complex models while maintaining low dimensionality and computational efficiency. In order to be effective for real-time control applications there are a few additional requirements for the chosen model. Namely, the model must support both future state prediction and an estimation of the future state uncertainty. These are necessary because the speed at which reactions and interactions happen in the human walking system is incredibly fast. It has been shown in Smeesters *et al.* (2001) that reaction time is directly related to a persons stability. Prediction capability will allow a future controller to make decision earlier such that when a specific position or force is necessary such as in a scenario where one looses their balance, the controller can act before it is to late. Estimation of future state uncertainty will give the ability to reason about how likely the current action is to lead to an undesired state. Additionally, the algorithm must have sufficient faculty to combine multiple modalities such as sensors and biomechanical features such that the model is sufficient to map from observed sensor data to unobserved data. Furthermore, the model should be able to model different types of human walking gaits such as walking on level ground, up and down slopes, or up stairs. How different the models are and what generalization capability exists in the generated models is an important question that will be addressed in the later portion of this dissertation. Lastly, the most basic component of bipedal walking is a cyclical or rhythmic structure, while the understanding of human robot interaction is one of individual discrete actions. All together, if real-time prediction is desired there are some significant barriers to its implementation.

Interaction Primitives have been used for human robot interaction for years and are able to deliver: predictions of future states with an estimation of uncertainty, estimations across multiple modalities, and generalizations to different spaces or trajectories. Also, Interaction Primitives are very fast in their prediction and estimation abilities and would therefore be an excellent candidate for this dissertation. However, Interaction Primitives lack a few important features to work well with human walking; namely due to the cyclic nature of walking. Traditional Interaction Primitives assume that a trajectory has a beginning and an end, and that and changes in the phase are monotonically increasing as seen in Figure 4.1. This trajectory will only lead to a single action, if the trajectory is to be used again then none of the information about the previous states will be passed into the next trajectory. This is not the case for cyclical human walking shown in Figure 4.2 below which repeats over and over. Repeating or non-monotonically increasing phase conditions in traditional Interactions Primitives will not work due to how the conditioning applies to future states. In order to transition traditional Interaction Primitives to work with cyclical trajectories I will investigate typical human walking behavior in order to create a novel approach to interaction primitives where the cyclical nature of walking is present in the phase estimation, basis structure, and conditioning.

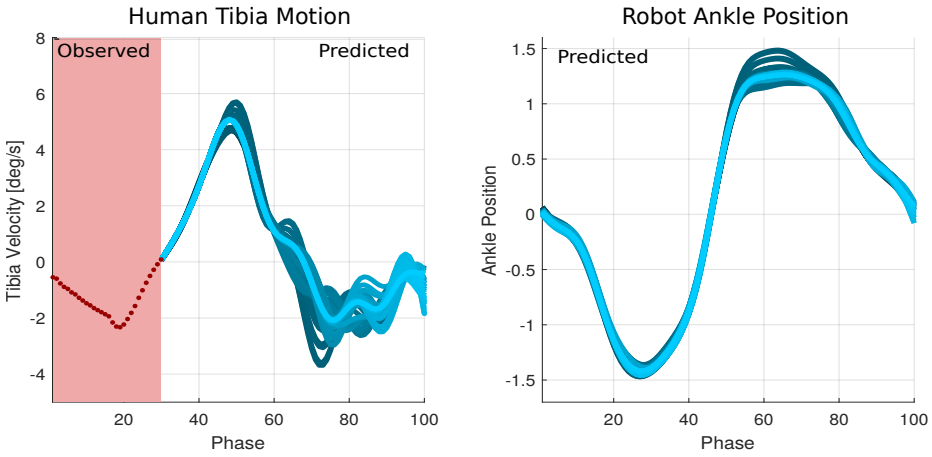

Figure 4.1: Probabilistic prediction of multiple variables as single trajectory.

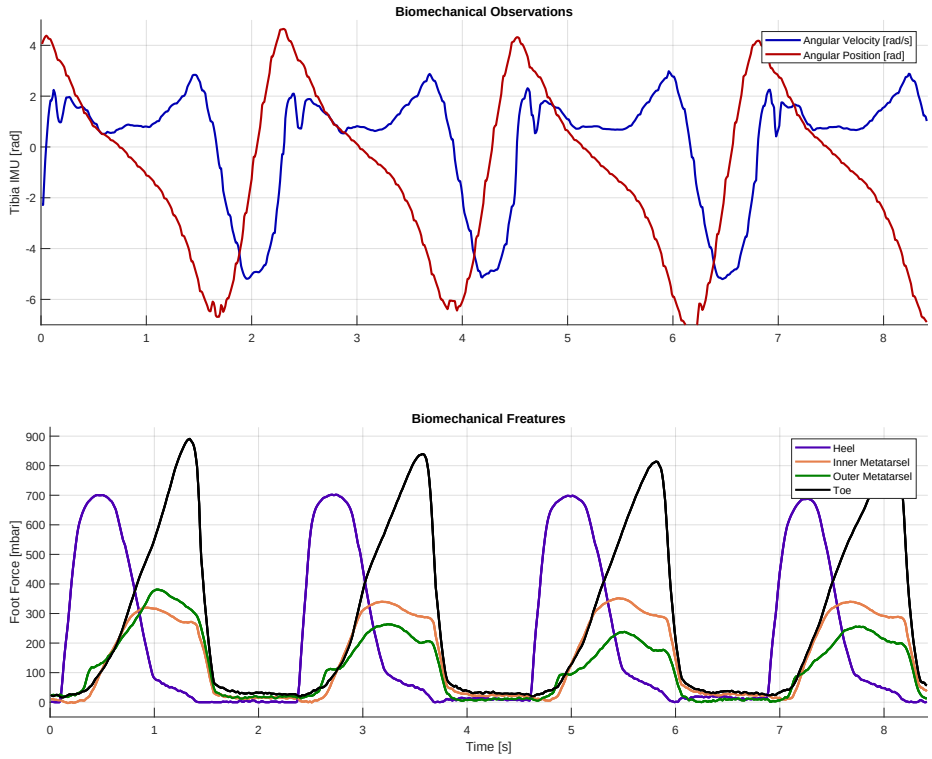

Figure 4.2: Example repeating walking cycle

4.1 Transitioning to Cyclical Interaction Primitives

In order to move from a trajectory space into a space where repetitive actions are available I took inspiration from biomechanical analysis of walking. Burgess-Limerick *et al.* (1993) discusses how complex joint movements within tasks such as walking or picking up items can be quantitatively described by phase plane evaluation. They show that phase angle analysis of multi-joint coordination is sufficiently sensitive to measure alterations in the task caused by changes in body kinematics or kinetics. By expressing joint positions, velocities, and loads on a phase plane the cyclic nature of this task becomes evident as a limit cycle. The limit cycle shown in Figure 4.4 below is formed by tibia angle and tibia angular velocity. This limit cycle has two main portions shown in Figure 4.3, the first of which starts at heel-strike, at this point in time the heel of the descending foot makes first contact with the ground and oscillates as the rest of the foot contacts the ground as well. This is the start of the stance phase where by bringing the foot under the body the center of mass is raised, in stance the Achilles tendon acts as a spring to store energy. The end of this phase and the beginning of the next is push-off where the Achilles tendon releases its stored energy pushing the raised body forwards and initiating the following swing phase. In the swing phase the leg uses mostly inertia from the push-off to return to a forward position ready for the next heel strike.

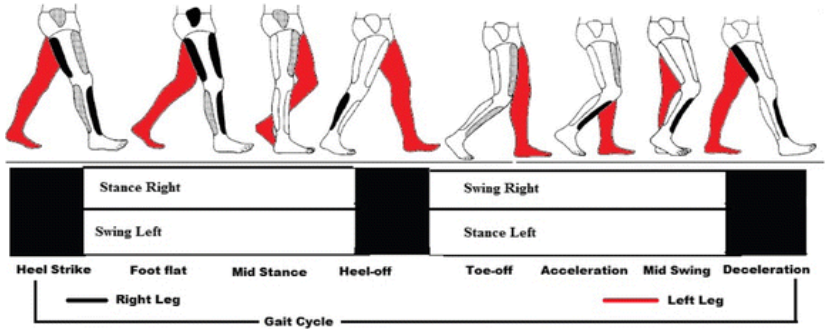

Figure 4.3: Human gait cycle during normal walking from Nandy and Chakraborty (2017).

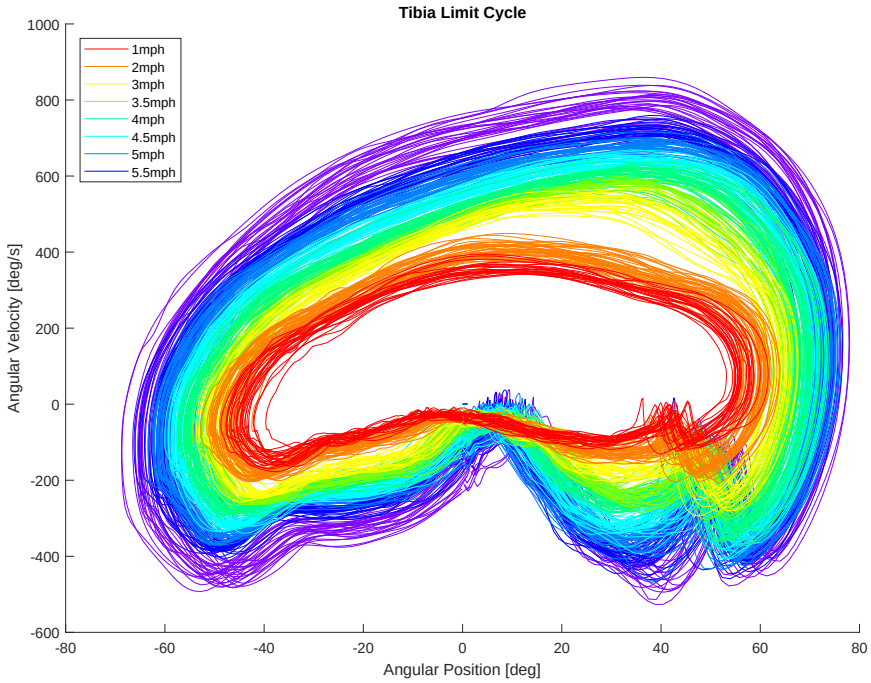

Figure 4.4: Limit cycle from tibia angular velocity and angular position at different speeds.

4.1.1 Phase Projection

In order to create a unified system around this Phase Plane method multiple changes will have to be made to the Interaction Primitives. Most important is the method used to get a continuous estimation of phase within this new space. Prior work in Interaction primitives has used methods such as DTW to achieve a phase estimation. DTW has a number of drawbacks; most notable is the fact it is an incredibly slow algorithm, it has a tendency to make random jumps, and it does not model well in a cyclical space. Other work has used SLAM functions to first localize within a space and then to map to the Interaction Primitive, this method is also computationally heavy and requires the entire DOF space to be mapped. A more optimal method is to use the advantages that the limit cycle imparts, by localizing on a single low dimensional Phase Plane. The simplest method of doing this is shown in Figure 4.5 below where within the limit cycle the angular component of the polar coordinates are used to generate a phase estimation.

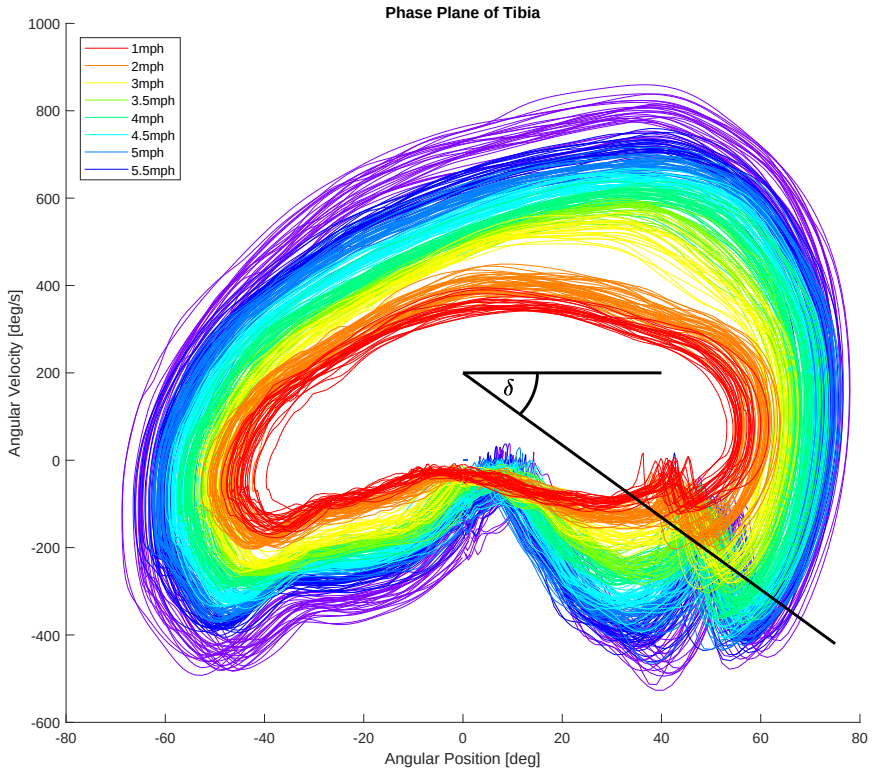

Figure 4.5: Limit cycle from tibia angular velocity and angular position at different speeds with basic phase estimation overlay method.

While this method seems fairly effective, unfortunately, it does not correctly map phase in a few areas of the limit cycle. These areas shown in Figure 4.6 below. The main problem areas are heel-strike and push-off where the polar angle does not line up across multiple observations. Matching phase across multiple demonstrations is incredibly important to the usefulness of the algorithm. When working with human subjects it has been found that one of the most important aspects human robot interaction in exoskeletons or prosthetics is the ability to match the human timing (Young *et al.*, 2017), (Sugar *et al.*, 2015).

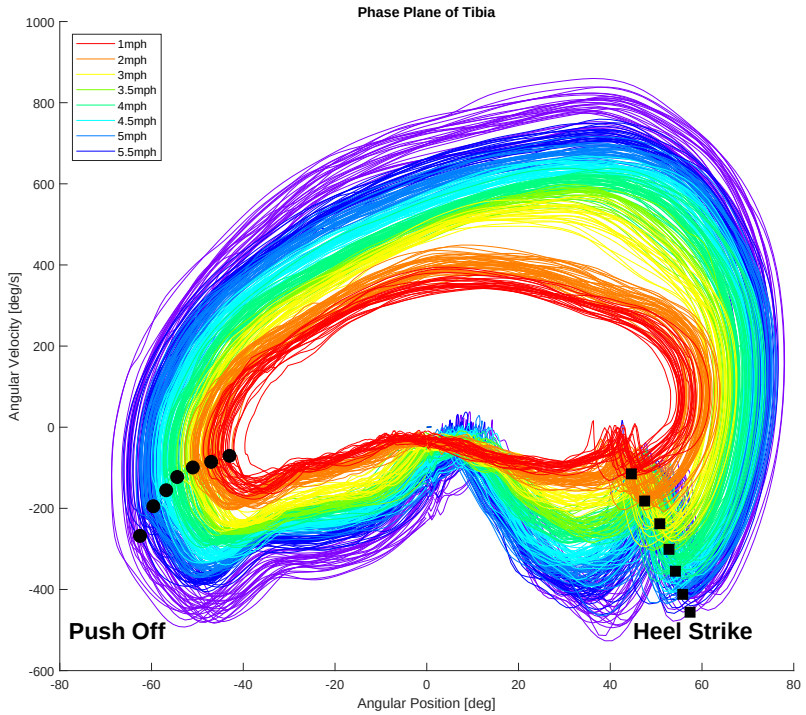

Figure 4.6: Limit cycle from tibia angular velocity and angular position at different speeds with points showing biomechanical features at each speed.

For the purpose of producing a more advantageous phase estimation, a novel approach of Phase Projection will be used to map individual biomechanical observations into the phase space. In Phase Projection the limit cycle is divided up into discrete phases by drawing lines through the biomechanical feature space of the observations, shown in Figure 4.7 below.

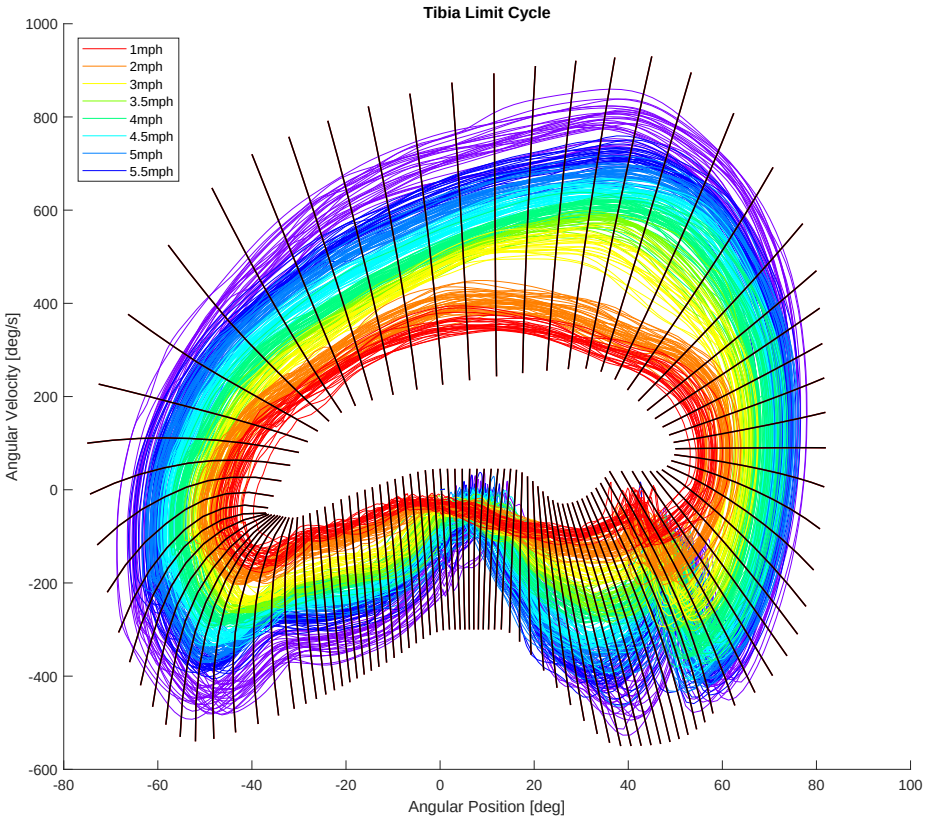

Figure 4.7: Expanded phase mapping across entire limit cycle.

Next, the biomechanical feature space is used to generate a three dimensional surface seen in Figure 4.8 and Figure 4.9 below, by creating a cubic interpolation between points. When a new observation is projected onto this surface it will map the observation from the limit cycle into the new phase dimension. This method of Phase Projection is computationally efficient and highly accurate because it relies on the assumption that the kinematics and kinetics of the human body are linked through the joint relationships. The proposed Phase Projection method creates a manifold which is cyclic in nature and can decompose any observation in the given limit cycle space into a estimated phase. This is an astonishingly efficient method for estimating phase.

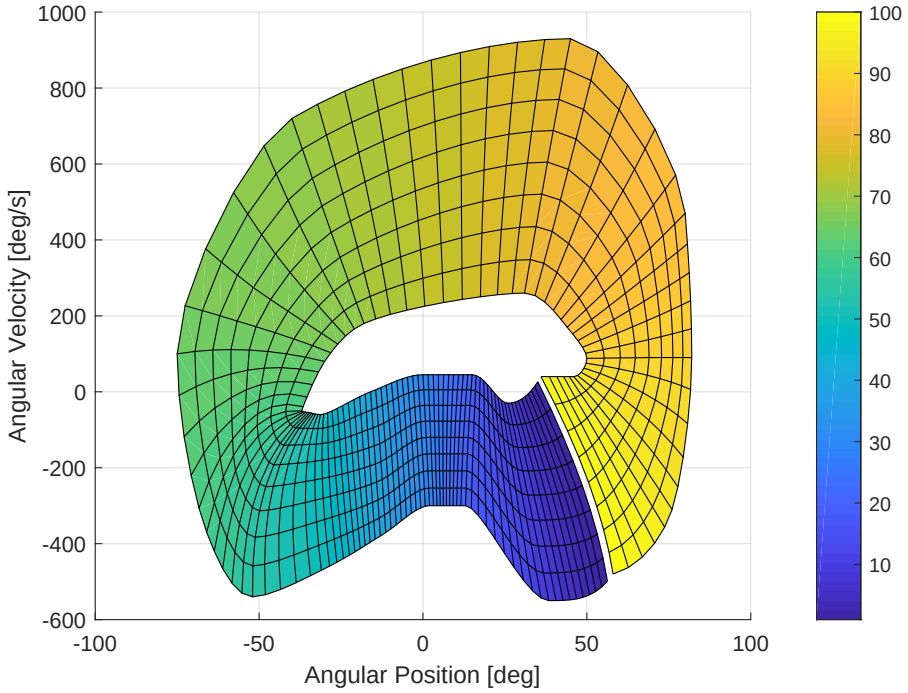

Figure 4.8: Phase Surface for phase projection in 2-dimensions.

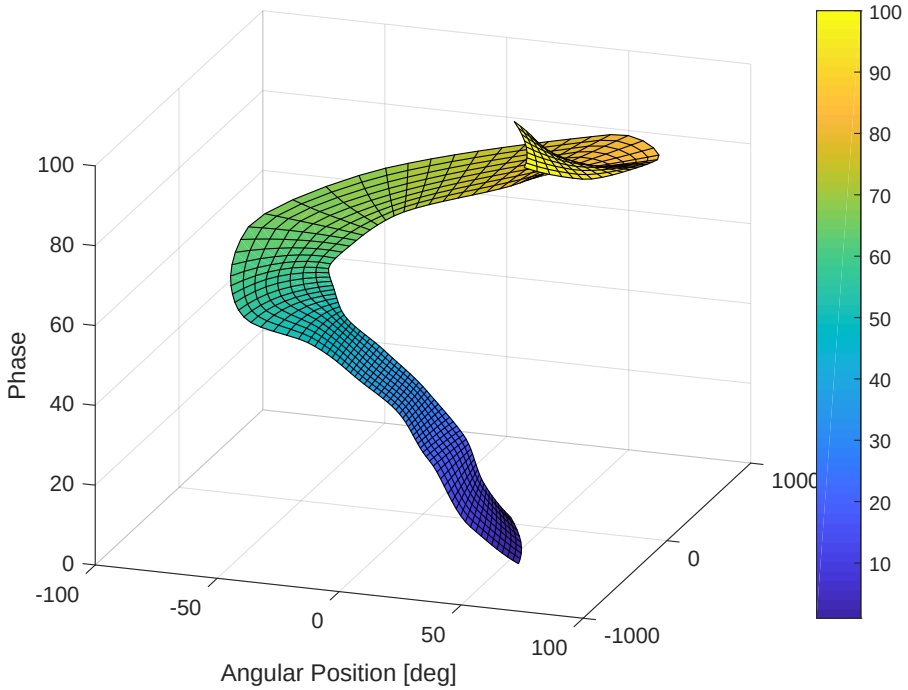

Figure 4.9: Phase Surface for phase projection in 3-dimensions.

4.1.2 Basis Functions

In typical Interaction Primitive methods basis functions are used in order to lower the dimensionality of the problem. For this to be effective the number of basis functions should be much less than the number of points in the trajectory in time. Dimensionality reduction remains effective because the typical basis functions are formed from Gaussian curves, where the mean of each Gaussian is shifted in phase to form a typical set shown in Figure 4.10 generated from Figure 4.11 below. Any trajectory is then decomposed into a set of weights on these basis functions like the one shown in Figure 4.12. The set of weights acts as smoothing function as it reduces the trajectory to a lower dimensionality, therefore the number of basis functions is indicative of the lever of accuracy desired in the reproduction seen in Figure 4.13.

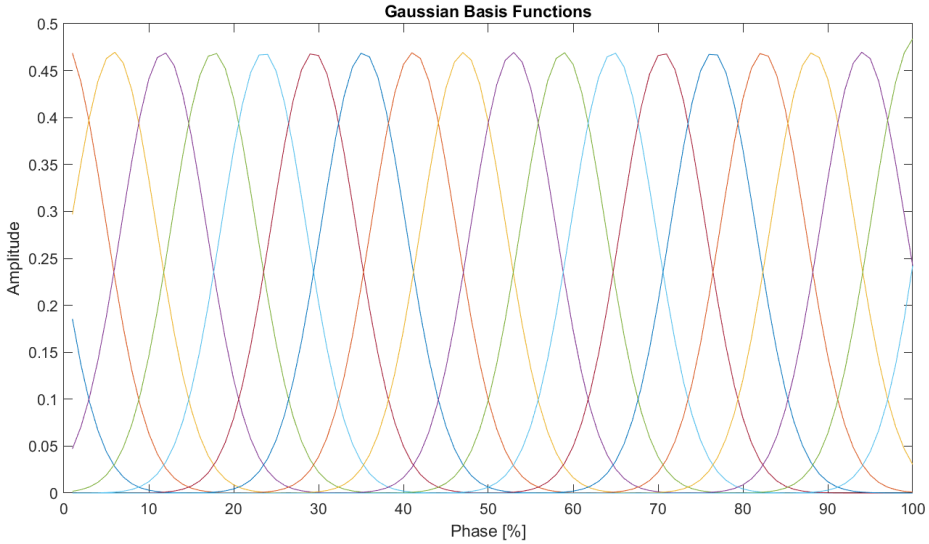

Figure 4.10: Phase Surface for phase projection in 3-dimensions.

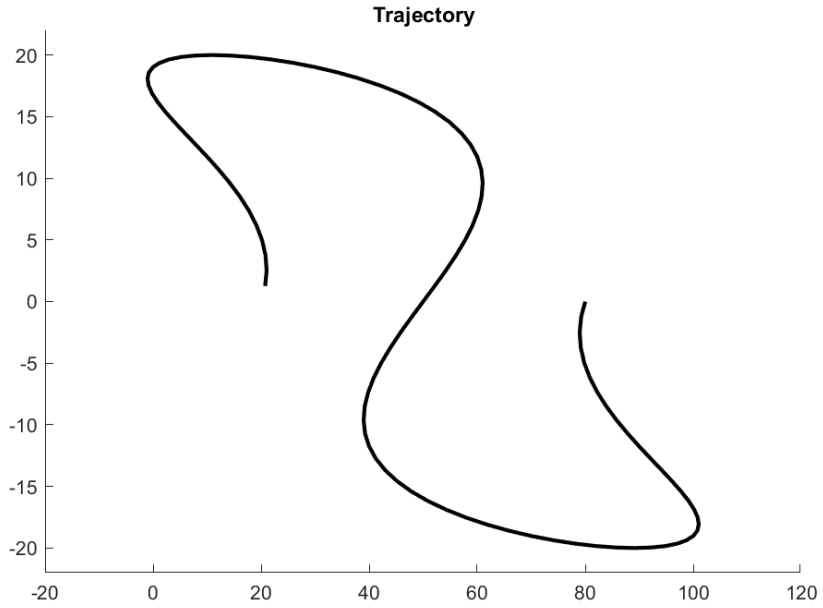

Figure 4.11: Phase Surface for phase projection in 3-dimensions.

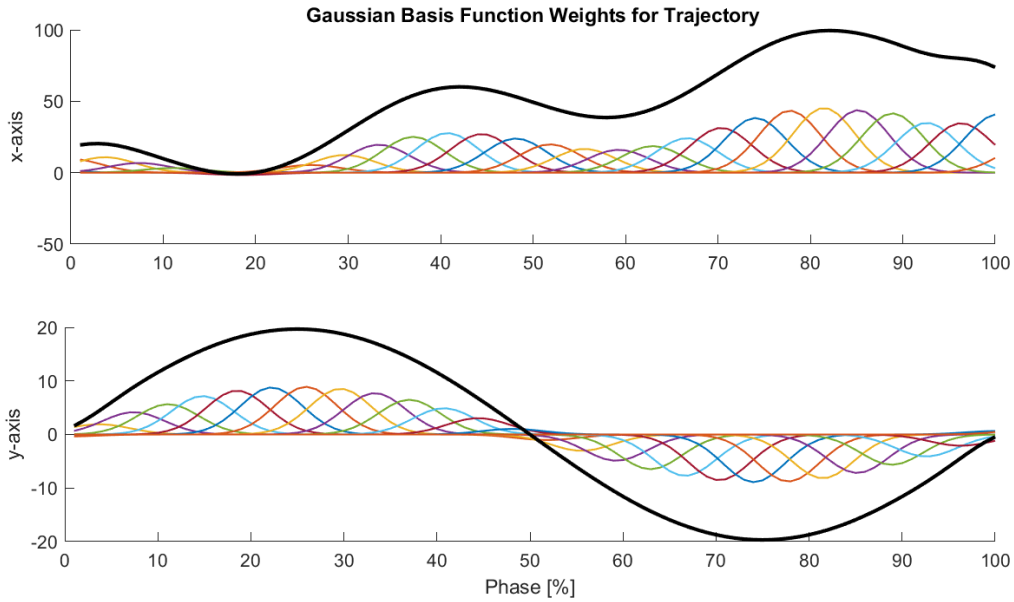

Figure 4.12: Phase Surface for phase projection in 3-dimensions.

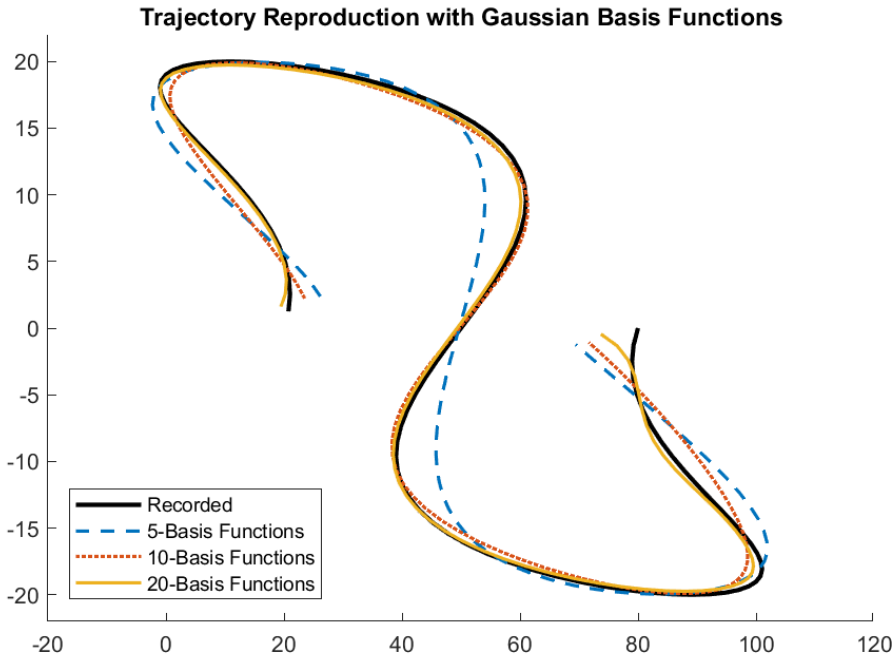

Figure 4.13: Phase Surface for phase projection in 3-dimensions.

Unfortunately, this traditional method does not account for cyclical or recurrent trajectories, they are instead designed to have a distinct start and end point. For the correlation analysis to work in the Interaction Primitives the basis functions must be moved into a cyclical domain. In a cyclical domain the functions would not have a beginning and end but rather wrap around such that it creates a cohesive cycle. I propose two methods for this cyclical basis functions: Sine series basis functions and von Mises basis functions.

Sine Series Basis Functions

Fourier series is an obvious choice when discussing functions that can approximate repeating sequences in a low dimensional space. The effectiveness of Fourier series to reproduce square, sawtooth, or any other repeating signal in electrical engineering is

well known. The Fourier series is able to represent a periodic function by decomposing that function into a possibly infinite set of oscillatory functions, such as sines, cosines, or complex exponentials. In this way the dimensionality reduction is done such that all power in frequencies above that of the highest frequency function in the Fourier series is lost. While there are a number of mathematical ways of calculating the exact Fourier series for any given function, since there is not specific function in this case but rather a collection of data the series will be attained numerically. Examples of the Series being used on a single dimension of some collected data is shown in Figures 4.15 and Figure 4.16 below. The basis function frequencies are limited to ones which match at the zero degree location on the polar plot. This means that the function will not have any gaps or jumps from one cycle to the next.

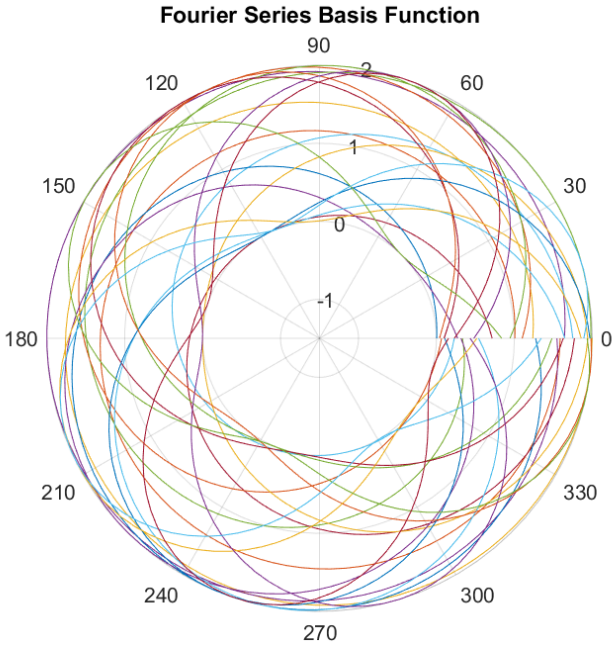

Figure 4.14: Phase Surface for phase projection in 3-dimensions.

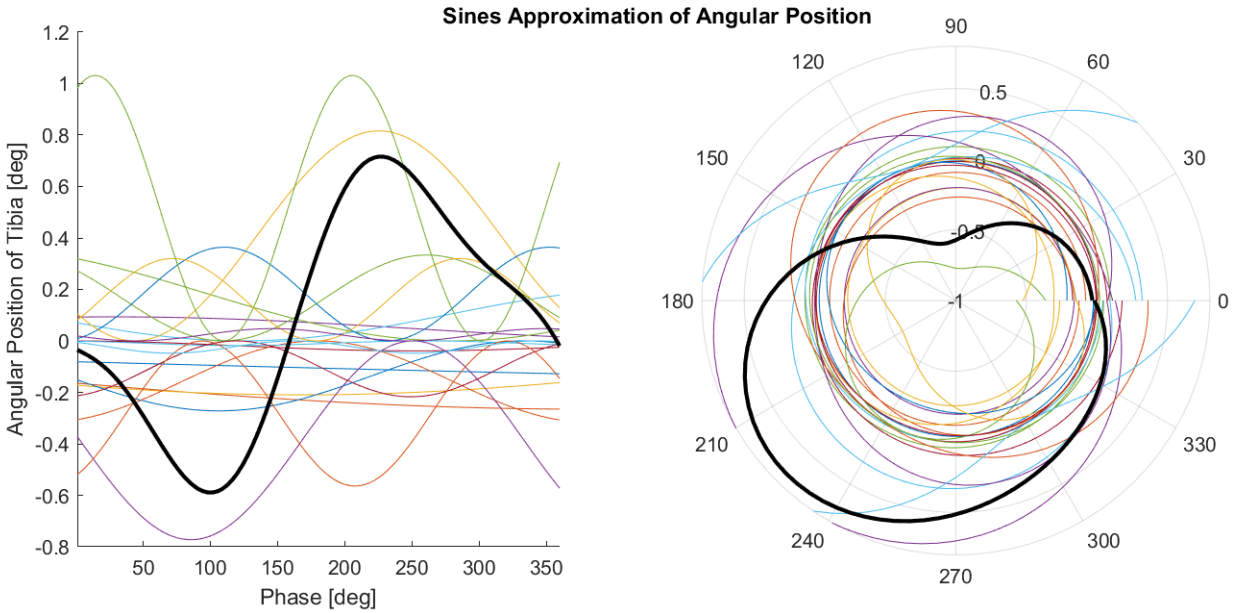

Figure 4.15: Phase Surface for phase projection in 3-dimensions.

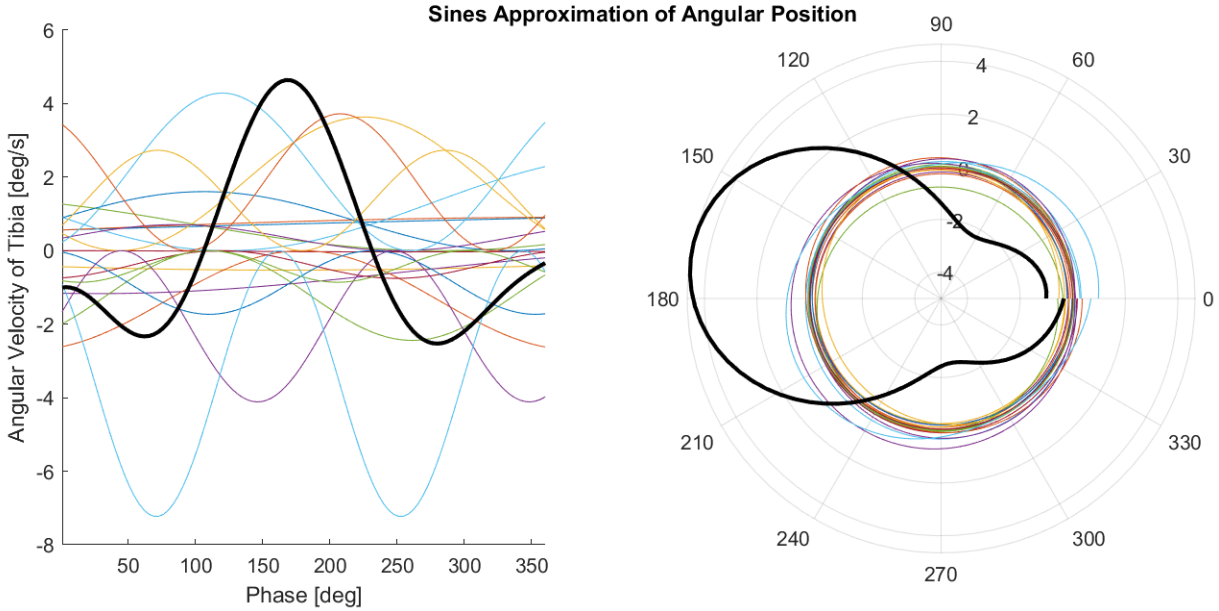

Figure 4.16: Phase Surface for phase projection in 3-dimensions.

von Mises Basis Functions

The von Mises distribution is a continuous probability distribution on a circle and is very similar to the Gaussian function. In fact, the von Mises distribution is a close approximation to a wrapped normal distribution. It was created as a stationary distribution of the drift and diffusion process on a circle, and is therefore intrinsic to the cyclical space this requires. The von Mises distribution is an excellent basis function for this work because both the mean and variance are controllable through the Probability Density Function(PDF)

$$f(x|\mu, K) = \frac{e^{Kcos(x-\mu)}}{2\pi I_0(K)}.$$

Where μ is the location of the mean of the PDF, K is the reciprocal measure of dispersion $1/K$ is comparable to σ^2. I_0 is the value of the modified Bessel function of order zero with the concentration parameter K:

$$I_0(K) = \sum_{i=0}^{\infty} \frac{K^{2i}}{2^{2i}(i!)^2}$$

An example of von Mises basis functions can be found in the polar plot of Figure 4.17. For the von Mises basis function, dimensionality reduction happens locally instead of on a frequency basis. The dimensions are reduced such that local changes in the function exist but are dependent on the number of basis functions and where they fall. One final thing to note is that some of the basis functions will extend beyond 0 or 360 degrees such that the space will not be separated at the 0/360 degree mark.

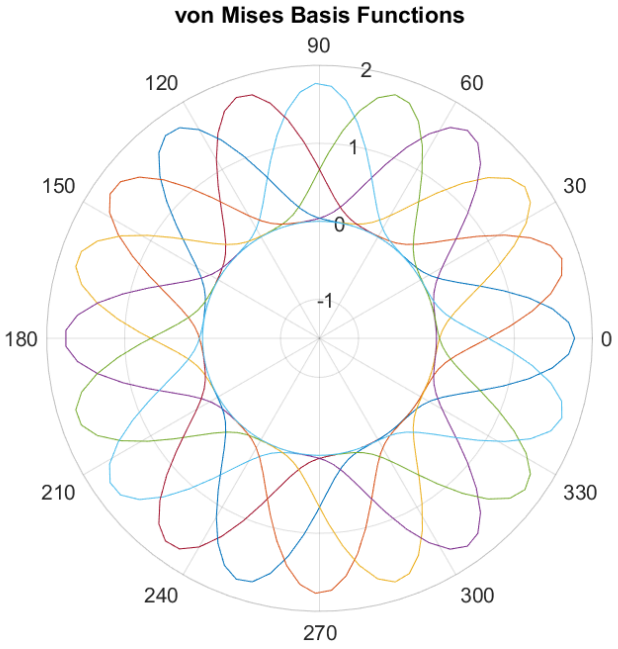

Figure 4.17: Phase Surface for phase projection in 3-dimensions.

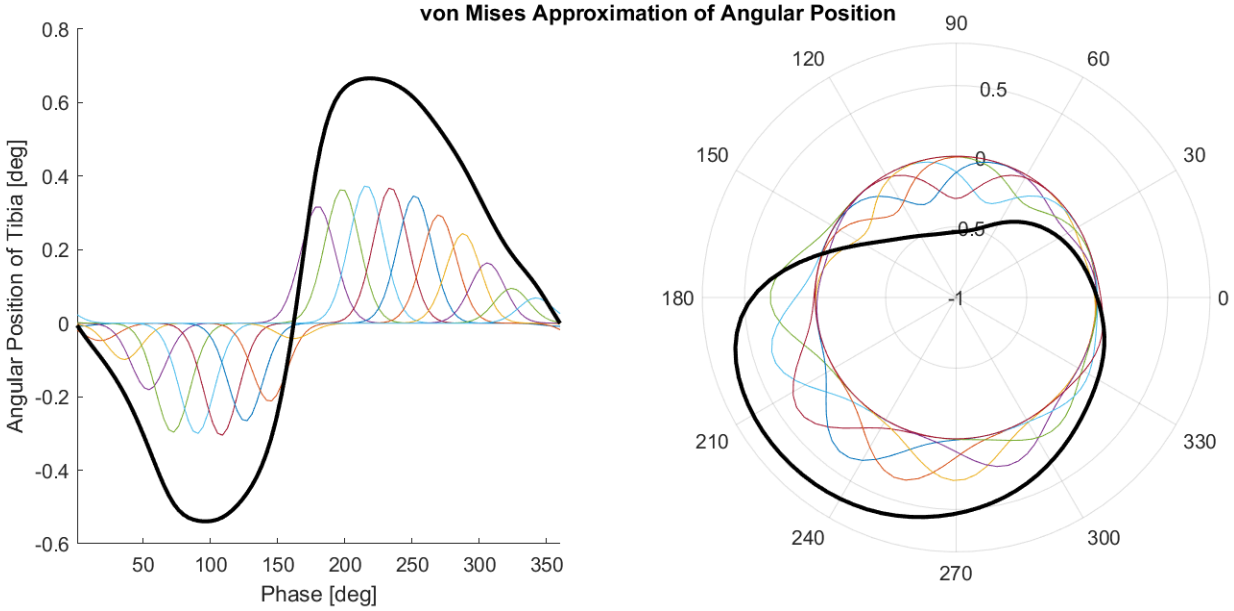

Figure 4.18: Phase Surface for phase projection in 3-dimensions.

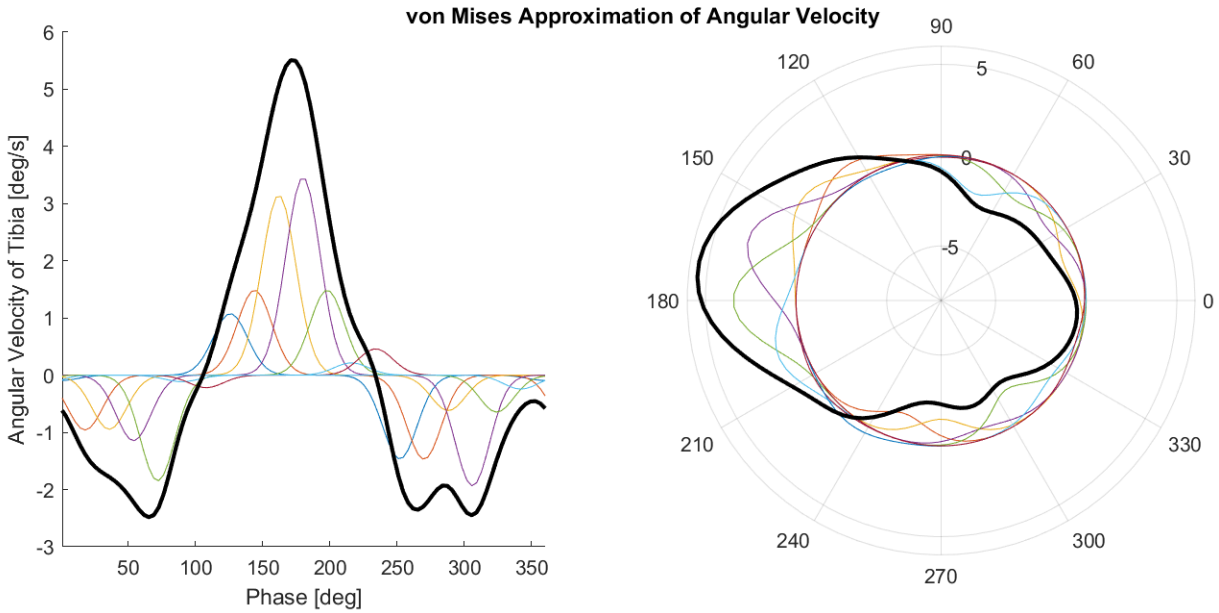

Figure 4.19: Phase Surface for phase projection in 3-dimensions.

Chapter 5

EXPERIMENTS

To thoroughly examine the effectiveness of these new methods for incorporating cyclical or repeating motions into Interaction Primitives a number of experiments were developed around the concept of human walking. As explained earlier, human walking contains complex symbiotic relationships between kinematics and kinetics. This work intends to learn the interactive relationship between the three dimensional kinematics of the tibia and the forces on the foot that accompany them. Usefulness of these tests are two-fold. First, it will prove that Cyclical Interaction Primitives are able to predict future states of recurrent systems accurately and efficiently. Second, it will show that Cyclical Interaction Primitives have the power to intuit future non-observed biomechanical state within a human system. Both of these reasons are key to the further development of Preventative Robotics proposed in the introduction. For most of the experiments the IMU sensors will be used as observed variables and the shoe force sensors will be seen as controlled or predicted variables.

The following is composed of a number of sections which describe in detail the experiment, how they were carried out, and the important results that came from them. Section 5.1 discuses that data that was used in the experiments, how it was obtained and any pre-processing of the data that was done. Next, Section 5.2 details basic analysis of the data to get a general idea for the modalities that are present as well as the importance of each variable to the prediction of the shoe forces. Section 5.4 examines the two proposed basis functions (series of sines and von Mises) and compares the two to determine which is better suited for probabilistically modeling in a cyclical space. Section 5.5, Section 5.6, and Section 5.7 examine the statistical

power of Cyclical Interaction Primitives on the task of walking on level ground, on slopes, and up stairs, respectively.

5.1 Data Collection

For the purpose of successful prediction on a human system a number of modalities were desired. It is well known that synergies exist within the human body and the synergies are stronger the closer the joints are together. For this reason, kinematic lower leg data (motion of tibia in space) was desired to form the basis of the interactions. Along with the tibia data, force measurements for the foot as the predicted variable were also imperative to have. To date, there has been a great deal of testing and data collection done in human kinematics and kinetics to analyze analytical solutions to the problem of human motion prediction and estimation. Therefore, previous works were analyzed to see if databases were available and had the requisite data for this dissertation's experiments. Unfortunately no cohesive data set was freely available that had the level of detail which was desired. The majority of the foot force data was extrapolated from force measurements on a split treadmill. While these treadmills produce very high quality data with many DOF, the treadmills are not able to tell which part of the foot is producing the force. If the biomechanical data is to be used in a real-time control strategy seeing the synergisms between forces on individual segments of the foot will be imperative to developing robust probability distributions. Additionally, the tibia data that was present was entirely 3D odometry data from motion capture cameras which would require a significant amount pre-processing to get into a usable state. For these reasons it was decided that the data should be captured specifically for this dissertation. In this way the sensors and data rate can be specified to fit optimally within the designed algorithmic setup.

The sensors chosen are the 9 DOF IMU Platform listed in Section 3.2 and the Shoe Force Platform detailed in Section 3.1. After careful consideration and some algorithmic tuning the data rate of each device was set to 100Hz. This rate was chosen based on a number of factors, but mainly due to the algorithmic bottleneck; 100Hz was the maximum speed at which the algorithm could consistently function without skipping over any data. Further work was not done to increase algorithm speed because 100Hz was determined to be an adequate speed to accommodate features within the walking and running trajectories. Having a constraint of 100Hz still allowed real-time functionality of the algorithm.

After mounting onto the body as detailed in Section 3.3, a majority of the data was collected on a treadmill with variable speed and slope settings. Individual trials were conducted for five minute intervals walking on the treadmill at varying speeds and inclinations to gather a substantial amount of data that can be used in analysis. In all, 20 trials were run on the treadmill by setting the speed to [1.8, 2.0, 2.2, 2.5, 3.0] mph and the angle to [-3.0, 0.0, 3.0, 6.0] % grade. Additional trials were done to gather stair data by finding the largest continuous staircase at Arizona State University and walking up it multiple times. Upon completion of the trials, the data was cut such that the dataset starts on the first step on the treadmill and ends on the last step. Further description of the data processing done can be found in each section below.

Sensor choice for the IMU made a big difference in choosing which data types to use in the algorithm. The IMU sensor is not the traditional paired accelerometer/gyroscope/magnetometer sensors, but also includes an on board microprocessor that uses the raw data to compute the quaternions of the sensor for every instant in time. This gave access to the raw data as well as world coordinate linear acceleration in 3 DOF and world coordinate angular positions in 3 DOF. It is a traditionally

frustrating problem to correctly and effectively integrate angular velocity from a gyroscope into position because small errors in the integration lead to drift overtime, so having the calculations done automatically is very useful. Since it is well known, see Section 2.5, that both tibia velocity and tibia position are highly related to foot pressure during walking the data types from the IMU that will be used are 3 DOF angular velocity, 3 DOF angular position, 3 DOF linear acceleration. Additionally, all pressure sensors on the shoes will be used.

Data from all sensor units was collected at the aforementioned rate of 100Hz. By keeping the rate the same between data collection and real-time testing, the algorithmic parameters such as noise do not have to be re-tuned. Also of note is only a single test subject was used in the entirety of this testing. While it is suspected that the learned models should transfer fairly well to other participants, Institutional Review Board (IRB) considerations restrained this testing until a future date.

5.2 Data Analysis

To get a good view of the data and to begin to form some opinions of how the interactions are formed within the human subject the data was put through a number of processing steps to view the data in different ways. Visualizing the data in a number of different ways will show features of the data that would otherwise be indistinguishable.

5.2.1 Principal Component Analysis

The first visualization method used is Principal Component Analysis (PCA) which is a statistical method that transforms data into a set of linearly uncorrelated variables. It does this in such a way that the variables are organized so that the first component contains the most variability (accounts for the largest amount information)

and the last variable contains the least variability. When used on a high-dimensional dataset it is often used to reduce the dimensionality, or to provide a low dimensional projection of the data viewed from the most informative direction. PCA components therefore illustrate how data within a dataset is related internally and to what degree. To use PCA in a way that reveals the internal structure of the subjects walking, it is used on the subjects self-selected speed of 2mph on level ground. Since PCA is sensitive to the scaling of individual variables the data was first normalized around each variables mean. This is not guaranteed to give an optimal result, as no optimal scaling rules have been found, but it should be efficient enough for this level of analysis.

Looking at Components

While getting a perfect result from PCA analysis is nearly impossible, a number of things can be shown from the PCA analysis. First, the analysis shows that the first four principal components account for 82.0% of the variability in the entire data set. This means that viewing four dimensions should provide a fairly accurate representation of the main relationships in the data. When these four principal components are plotted as in Figure 5.1 it can be seen that there are two different types of relationships. The first and strongest relationship is quite nearly circular; the relationship between components one and two clearly represents cyclical data within the dataset. This circular relationship is also present between components three and four; though, as expected of later components the data is not as well defined as can be seen in the first two. Within the data a second type of relationship can also be seen which is a cyclical relationship with a doubled frequency in one direction. A relationship of this type looks like a figure-eight on Figure 5.1 and represents the binary relationships that exist due to two legs walking at once. PCA analysis of this type provides strong

evidence that Cyclical Interaction Primitives have merit in this application. Since the strongest principal component is cyclical it makes sense to base the model around the circularity of the data. Likewise, it shows that it is imperative to properly model the relationships within the space because some relationship have a doubled frequency component.

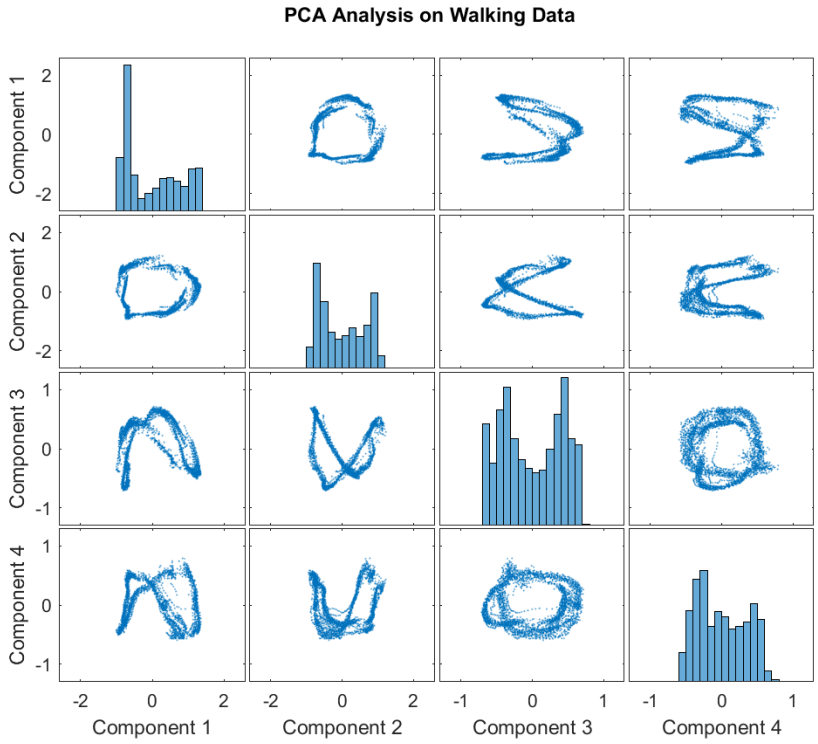

Figure 5.1: Four largest principal components from PCA analysis on level ground walking at 2.0mph.

Looking at individual variables

PCA analysis is so powerful because it delivers the Eigen Vectors along with the percentage of the variability that is explained by each component. From this information it is possible to calculate the explanative power of each variable on the variability from the PCA. Figure 5.2 plots each variable from all sensors against its

percent of explanation. By plotting the data in this manner it is possible to see which variables explain the most variability and which explain the least. Accelerometer data is by far the lowest of all the data. This makes sense due to the high frequency nature of accelerations at the tibia. Next lowest are the angular velocities in the Y and Z directions which can be explained by seeing that this data is most variable during swing when it is the least important to the step. Finally, all around at the same level are angular position in all three directions, angular velocity in the x direction and all of the forces at the foot. Between these eight components they explain 82.5% of the variability in the data. As a significant portion of the variability, it can be inferred that these variables will be the most important in the Cyclical Interaction Primitives. These variables clearly have the most power to explain the variability. However, it should be noted that this does not mean the data is correlated in this manner. Principal components are by definition linearly uncorrelated to one another and therefore caution should still be taken when trying to form statistical models around this data.

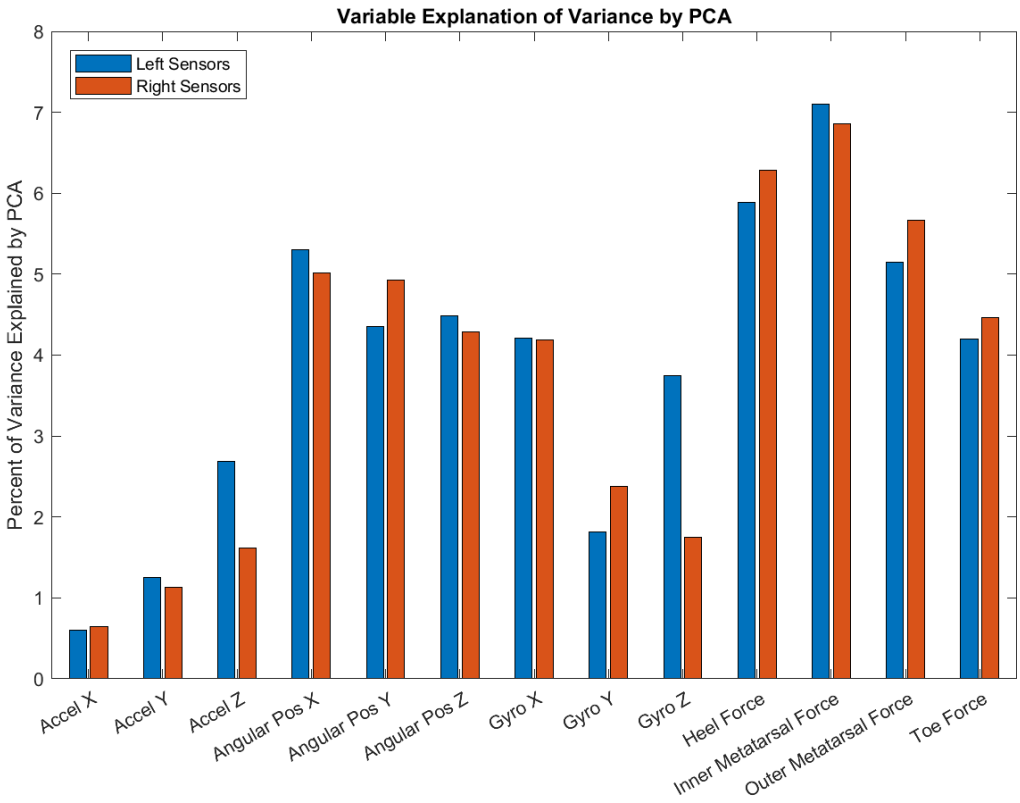

Figure 5.2: Percent of total variance explained by each variable from PCA Analysis on Level Ground Walking at 2.0mph.

5.3 Phase Projection Analysis

Before going any further the phase analysis is important to review and analyze to ensure it is functioning as intended. A trial of data was run through the Phase Projection method; to test the method itself the output was viewed in two ways: projection analysis and phase coherence.

5.3.1 Projection Analysis

First, each individual point from a single step is projected onto the phase plane. As a result, another layer of dimensionality to the data such that the efficacy can be viewed in two and three dimensions demonstrated via Figure 5.3 and Figure 5.4.

It is important to note that there are no jumps in the data in the phase dimension. The phase projection method used can easily remap from 100% to 0% phase, which is a significant issue with traditional methods. The cyclical nature of the phase projection method eliminates the need to time intensive algorithms such as Dynamic Time Warping (Sakoe and Chiba, 1978), or a particle filter.

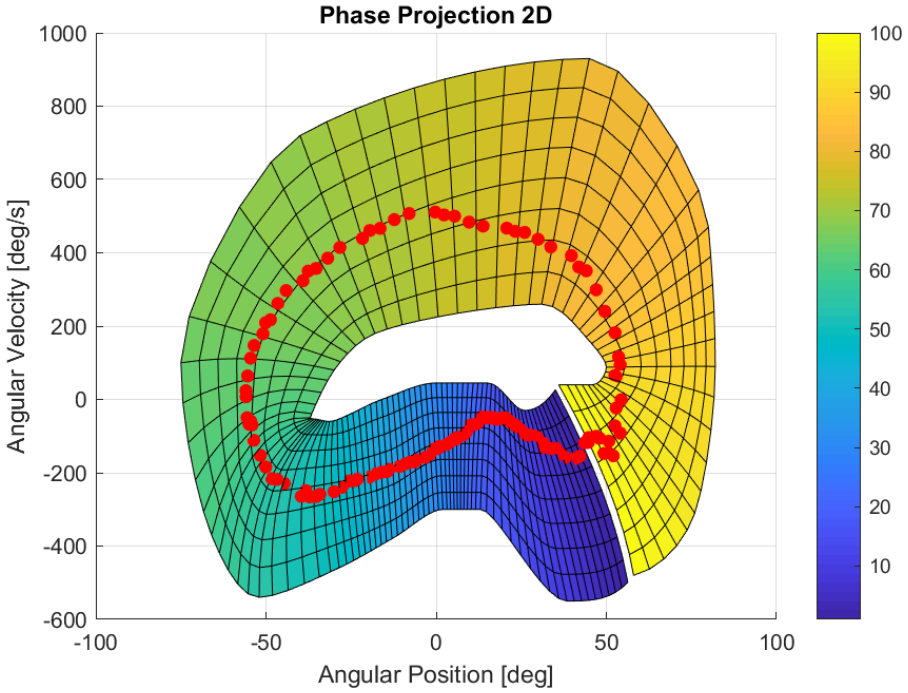

Figure 5.3: Data in red is projected onto the two dimensional phase plane in order to map the data into the phase dimension.

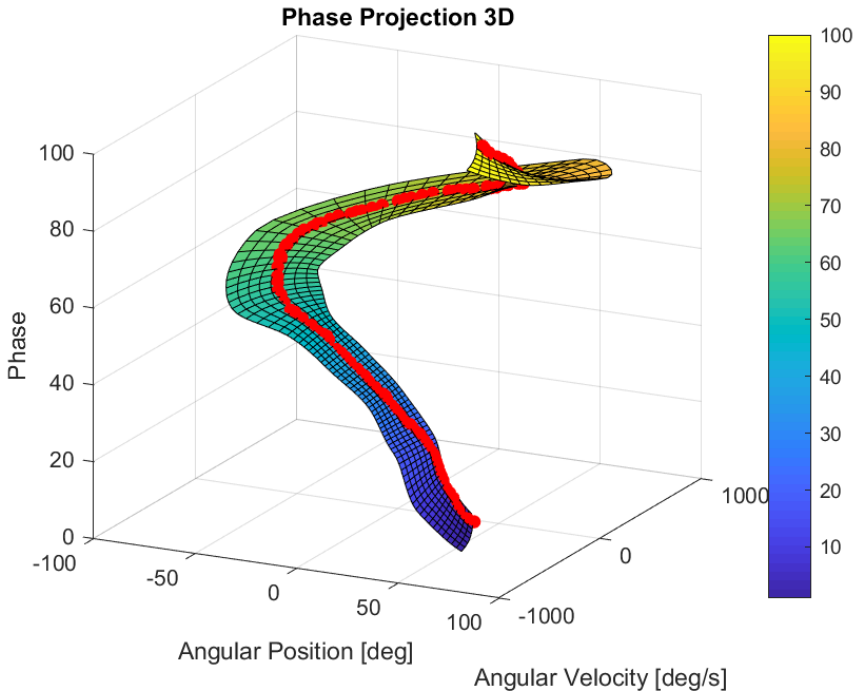

Figure 5.4: Data in red is projected onto the three dimensional phase plane in order to map the data into the phase dimension.

5.3.2 Phase Coherence

Even if transitions between points are smooth in the phase dimension the real question is, are they consistent? If points that share fundamental features in the biomechanical space, such as heel strike or toe-off, are not mapped together in phase then the data can not be said to be coherent in phase. Instead, coherence implies that biomechanical features are mapped together in phase. This is especially important because biomechanic feature prediction is the ultimate goal. In order for interaction primitives to work best they require accurate measurements of the variance at each point in phase. If biomechanical features are not mapped properly the underlying distributions built in Interaction Primitives will provide inaccurate predictions later on.

Table 5.1: Feature Coherence Evaluation

Feature Type	Mean Phase Location	Phase Variance
Heel Strike	0.11	0.56
Max Pushoff	54.6	1.15

To view the phase coherence a single trial of 23 steps at the self-selected speed of 2.0mph on level ground was mapped into the phase dimension using the Phase Projection method. Then the data was post processed to cut up and plot the trajectories of tibia angular velocity, heel sensor force, and toe sensor force. Next, force sensor data was compared to the phase information such that exact location of individual features could be pinpointed. The mean and variance of these features, plotted in Table 5.1. Figure 5.5, Figure 5.6, Figure 5.7, were used to evaluate the efficacy of the phase projection in regard to coherence. Variance of the location of actual heel strike in phase and variance of the location of maximum toe force in phase are two critical values to measure coherence in this case. As seen in Table 5.1, both of these values are around 1% which is excellent.

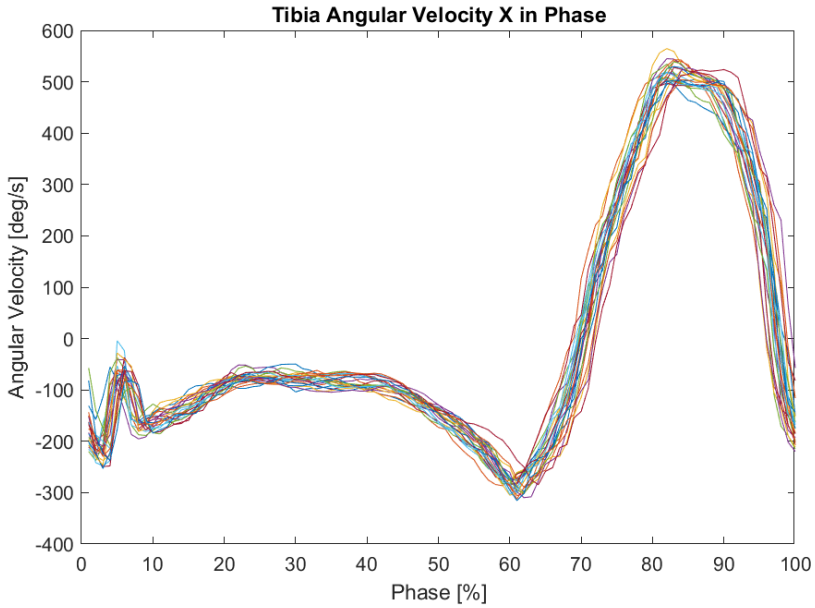

Figure 5.5: Angular velocity plotted against phase after Phase Projection method was used to align trajectories in phase.

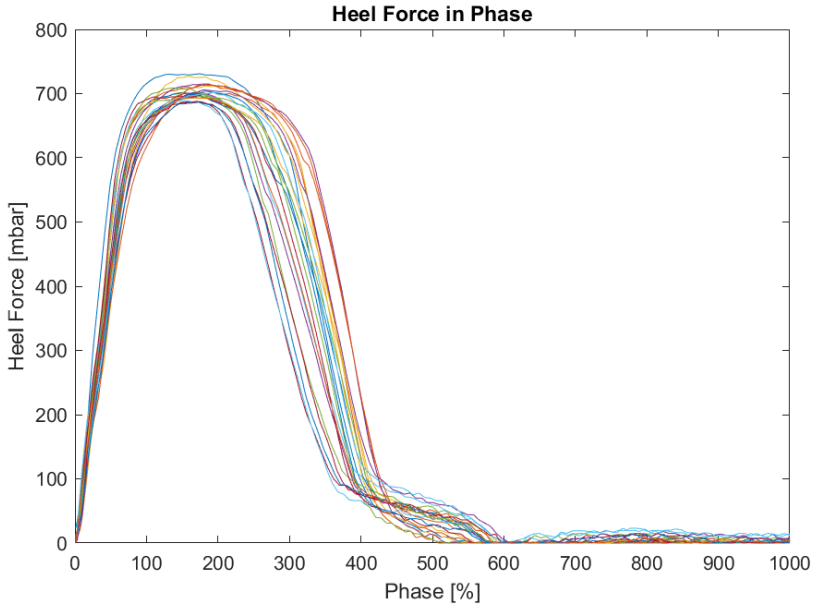

Figure 5.6: Heel force plotted against phase after the Phase Projection method was used to align trajectories in phase.

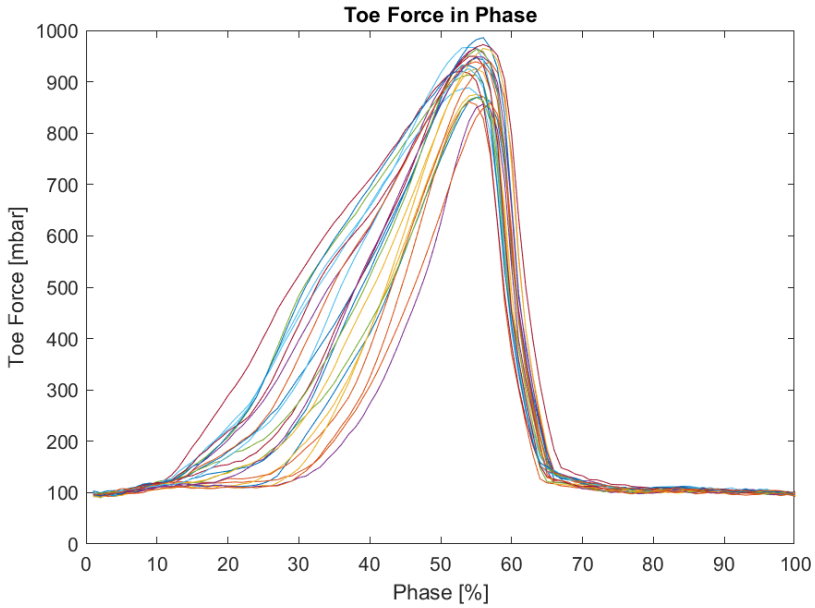

Figure 5.7: Toe force plotted against phase after the Phase Projection method was used to align trajectories in phase.

5.4 Basis Function Comparison

For the purpose of to moving further into the creating optimal models from the data, it is important to first evaluate the proposed basis functions and to choose a single one for the following experiments. This section includes information on the testing process, methodology, and outcome of the analysis done on the series of sines and von Mises Basis functions, to determine which one is better at regressing distributions of cyclical data.

The criteria being examined in the following Sections is (a) ability to accurately reproduce the mean of a set of trajectories (B) ability to accurately reproduce variance of a set of trajectories (C) ability to handle circular distributions. If these four criteria are not met then the basis function cannot be said to be useful for circular distributions. The following two Sections 5.4.1 and 5.4.2 analyze both of the proposed basis functions against one of the given criteria.

5.4.1 Reproduce Mean of Trajectories

Being able to reproduce the mean of a set of trajectories is fundamental to the effectiveness of a basis function in Cyclical Interaction Primitives. As the mean is used later in the Kalman filter step the accuracy of the mean is of vital importance. For the mean to be decomposed accurately into a set of weights shows that the lower dimensionally of the basis functions is sufficient to handle the data. Additionally, the ability to handle recursive distributions should be thoroughly examined. A cyclical basis function should have no true beginning or end, but rather be a constant continuation of the distribution.

With the intention of testing the accuracy of the two types of basis functions two data types should be sufficient; one from angular velocity and one from angular position. The chosen variables are angular velocity in the x direction and angular position in the x direction. Each of these variables have been reproduced in the right plots of Figure 5.8, Figure 5.9, Figure 5.10, and Figure 5.11 below.Additionally the Table 5.2 shows the mean squared error and mean absolute percent error of each data type on reproducing the mean of the trajectories as well as the percent discontinuity between 0° and 360°. Any discontinuity that exists will be effected by changes in distribution is undesirable. For the purposes of this testing the trial at the subjects self selected speed of 2.6mph on level ground was used. In total the entire trajectory consists of 25 steps.

Table 5.2: Trajectory Reproduction Error

	Angular Position	Angular Velocity
von Mises	MSE: 0.13 MAPE: 1.18% gap%: 0.00	MSE: 101.31 MAPE: 4.66% gap%: 0.00
Sines	MSE: 1.41 MAPE: 14.66% gap%: 1.96%	MSE 56,866 MAPE: 18.78% gap%: 0.75%

Between the mean squared error and mean absolute percent error it is clear that the von Mises basis functions far out perform the Sines. The feature accuracy is really the shining star of the von Mises functions as was expected of a local basis function type as compared to the global basis function type of the Sines functions. The ability to create local features without affecting the rest of the cycle was a tremendous benefit. With about 15% and 19% average percent error the sines basis function were neither incredible accurate globally nor did they have the requisite features to be accurate locally. It is also important to note that while the von Mises functions form a continuous trajectory in phase the Sines functions contain a discontinuity at the 0° mark. This junction is important because a discontinuity means that the distribution will not be effectively transfered across heel strike to the next step. Since the heel strike feature is the most important to be able to predict across will, due to prediction of trips or sudden steps, a discontinuity at this location would be very disadvantageous to the model.

5.4.2 Reproduce Distribution of Trajectories

Even more important than accurate reproduction of the mean to Cyclical Interaction Primitives is that ability to learn the distribution of the weights of the basis functions. Learning an accurate representation of the distribution will allow the model to have an understanding of the relationships between variables. As one variable changes with regard to the mean the model will be able to expect changes in other variables through the learned relationship. Since Cyclical Interaction Primitives utilize Gaussian distributions, looking at how the variance is modeled by the basis functions will give an indication to the efficacy of each basis function type.

Testing of each basis function type and how it handles variance and the re-currency of cyclical distributions was done by the same methods as in Section 5.4.1. The left plots of Figure 5.8, Figure 5.9, Figure 5.10, and Figure 5.11 illustrate the distributions of the weights and how they influence the overall generated mean trajectory. In these figures the standard deviation of each weight on the basis function is shown as the thickness of the basis functions $\pm\sigma$ and the standard deviation of the mean trajectory is shown as the gray thickness line around the mean also $\pm\sigma$. While the von Mises functions act as expected the Sine function generate a considerable standard deviation on the individual weights which is magnified in the mean trajectory. Since the sine waves act over large portions of the phase the standard deviation must be large in order to achieve the desired local features. Unfortunately this means that the relationships between weights is going to be odd and quite possible useless due to the extreme size. Overall, the sine basis functions make for a unreliable basis function source for Cyclical Interaction Primitives.

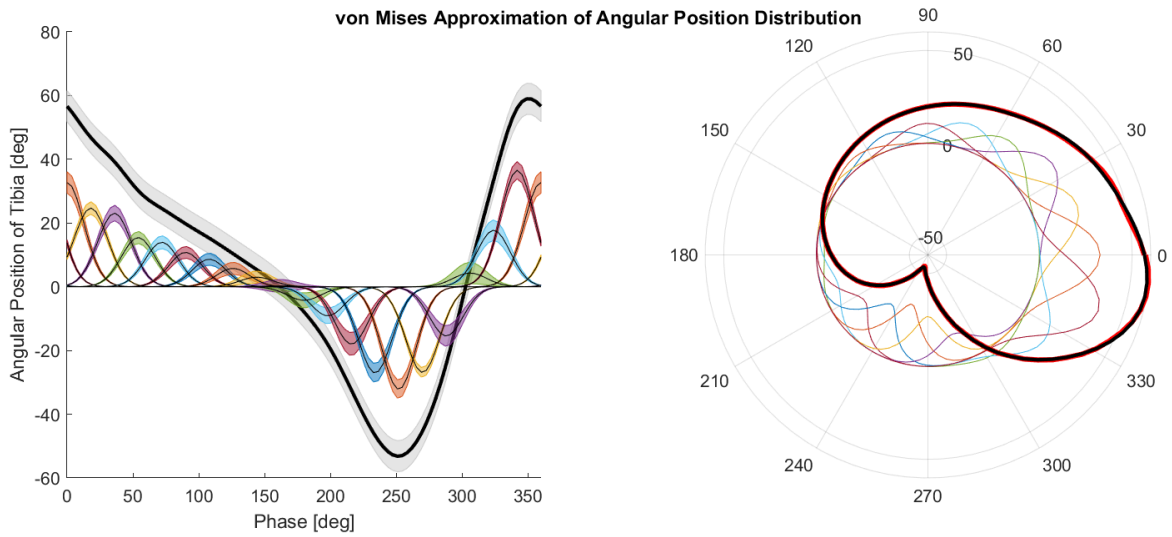

Figure 5.8: Left: Colored regions show the standard deviation of the von Mises basis function weights with the mean distribution trajectory of angular position in black. **Right:** Colored lines show the mean values of the von Mises basis functions with mean distribution trajectory of angular position in black compared against actual mean trajectory of observations in red.

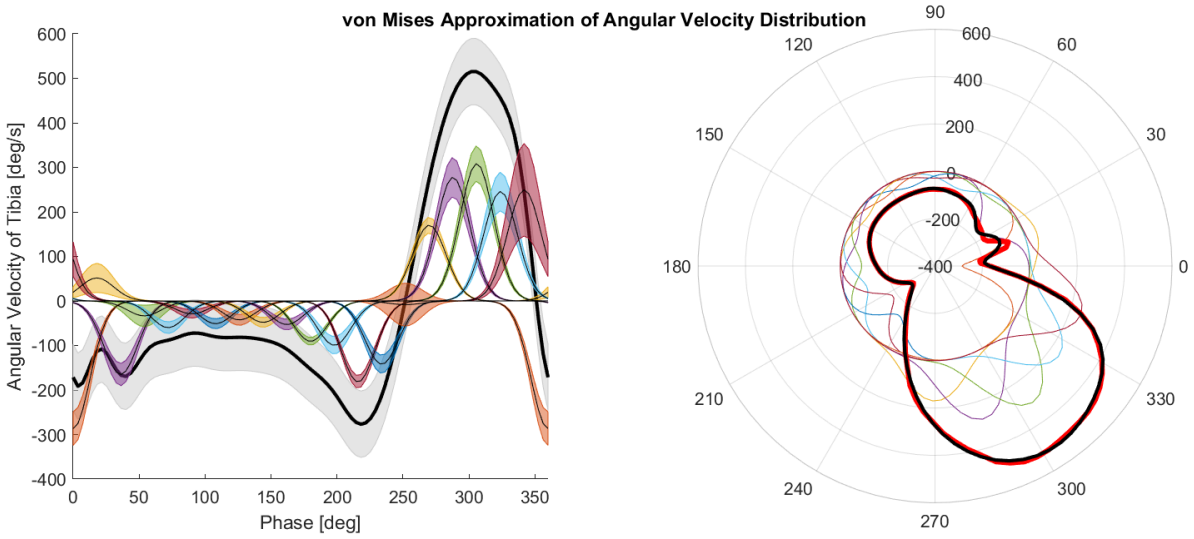

Figure 5.9: Left: Colored regions show the standard deviation of the von Mises basis function weights with the mean distribution trajectory of angular velocity in black. **Right:** Colored lines show the mean values of the von Mises basis functions with mean distribution trajectory of angular velocity in black compared against actual mean trajectory of observations in red.

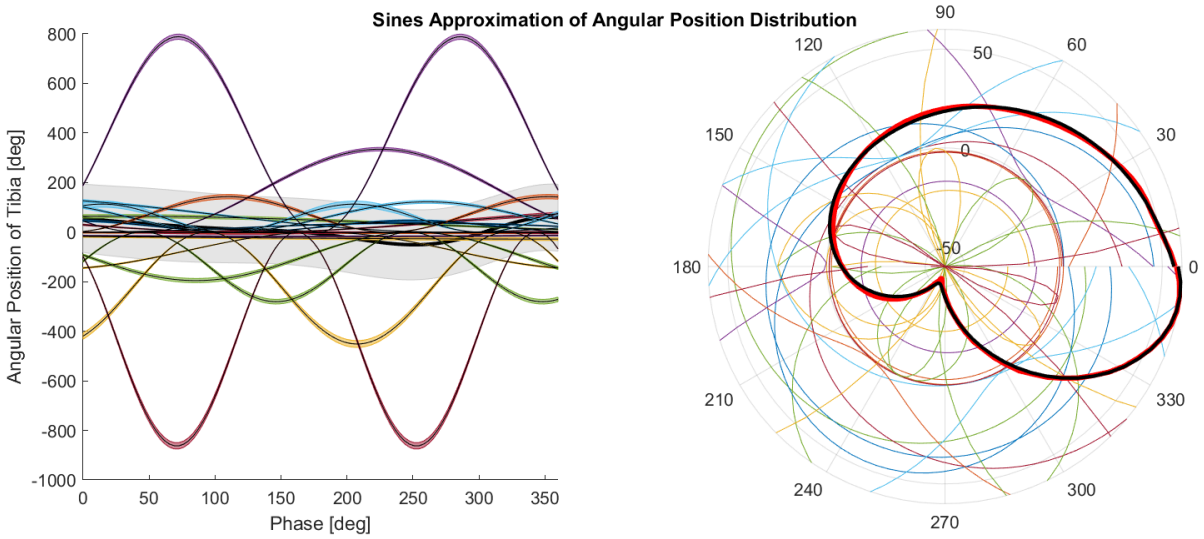

Figure 5.10: Left: Colored regions show the standard deviation of the Sine basis function weights with the mean distribution trajectory of angular position in black. **Right:** Colored lines show the mean values of the Sine basis functions with mean distribution trajectory of angular position in black compared against actual mean trajectory of observations in red.

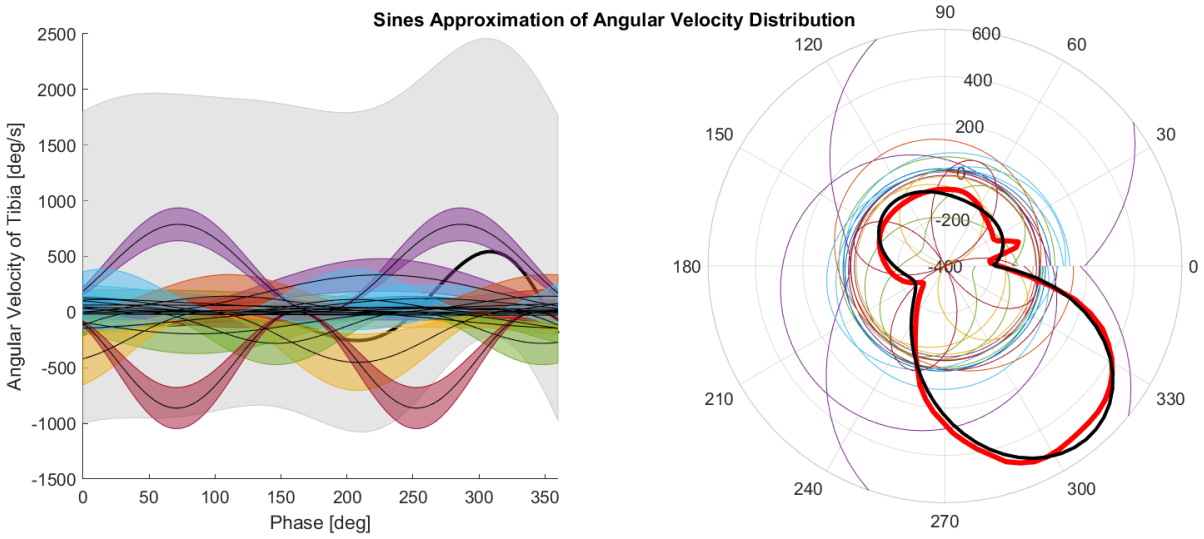

Figure 5.11: Left: Colored regions show the standard deviation of the Sine basis function weights with the mean distribution trajectory of angular velocity in black. **Right:** Colored lines show the mean values of the Sine basis functions with mean distribution trajectory of angular velocity in black compared against actual mean trajectory of observations in red.

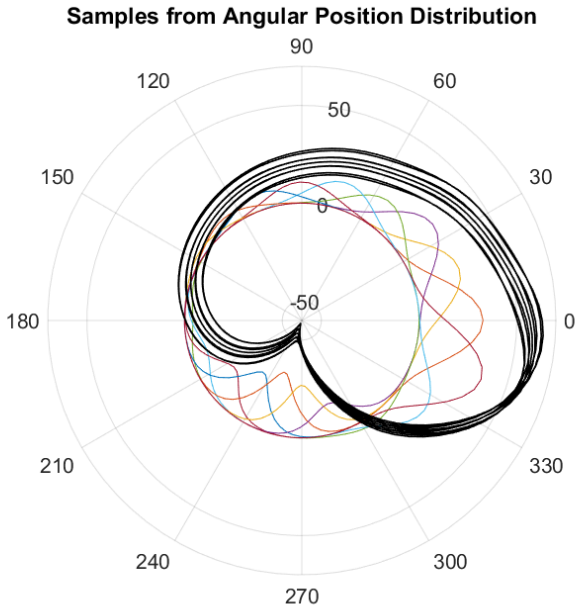

Figure 5.12: Samples taken from the distribution around the mean trajectory of angular position.

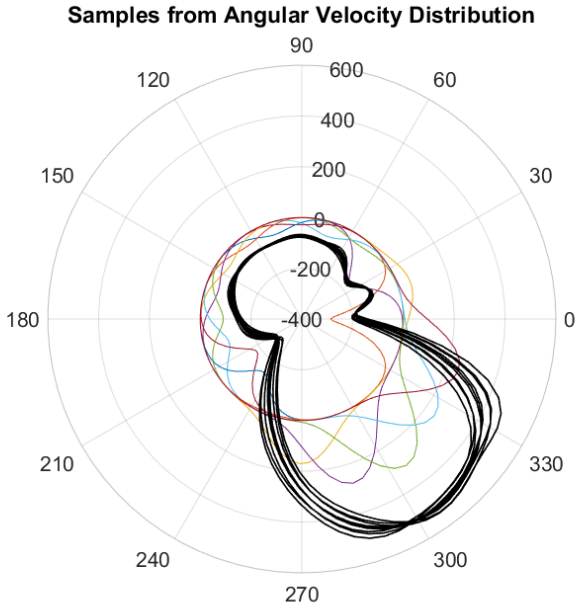

Figure 5.13: Samples taken from the distribution around the mean trajectory of angular velocity.

5.5 Learning Level Ground Interactions

Level ground walking is the most common of all gait tasks. As seen in the above section level ground walking can be efficiently modeled with cyclical interaction primitives in order to create a cohesive distribution that can estimate current states and predict future states. In this section the cyclical interaction primitives, utilizing Phase projection and von Mises basis functions will be tested on level ground walking in order to test the efficacy at predicting biomechanical features.

For this test a single trial of level ground walking on a treadmill at 3.0mph for five minutes was used. The trial was broken up into two portions such that the first 70% of steps collected during the testing was used for the learning step of Cyclical Interaction Primitives and the final 30% was reserved for the testing step. For this experiment the observed variables that the Cyclical Interaction Primitives are conditioned upon are angular position in 3DOF and angular velocity in the x direction, and the controlled variables of the Cyclical Interaction Primitives are the four foot forces which will be predicted. Even though real-time processing of the interaction primitives is possible the data was collected separate from the conditioning and testing step.

Results of the testing can be seen in the Table 5.3

Table 5.3: Level Ground Walking Prediction Errors

	Immediate Estimation	Prediction
MSE	0.11	0.56
MAPE	54.6	1.15

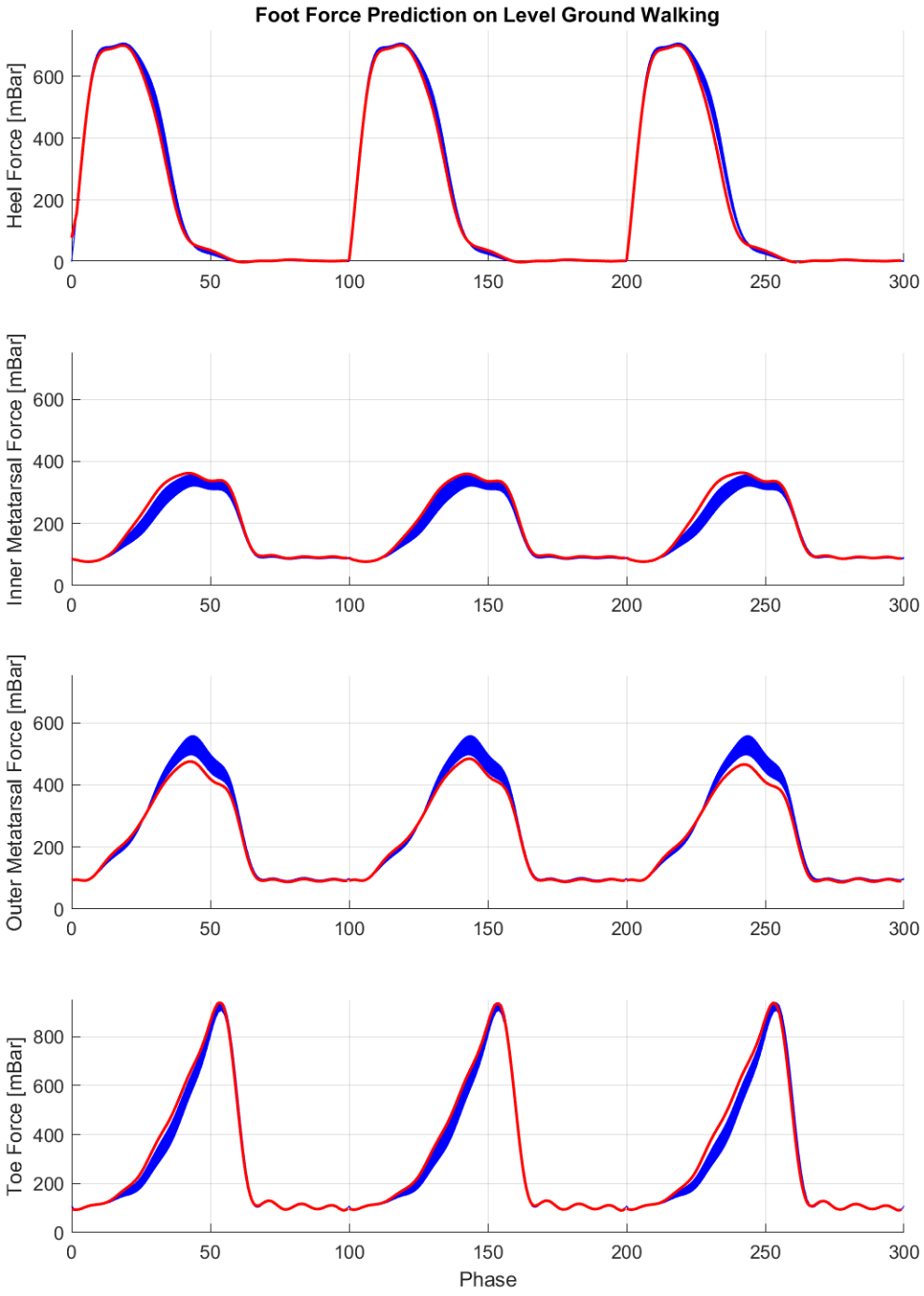

Figure 5.14: Red: Individual foot force predictions for a single step vs **Blue:** foot force standard deviations for level ground walking.

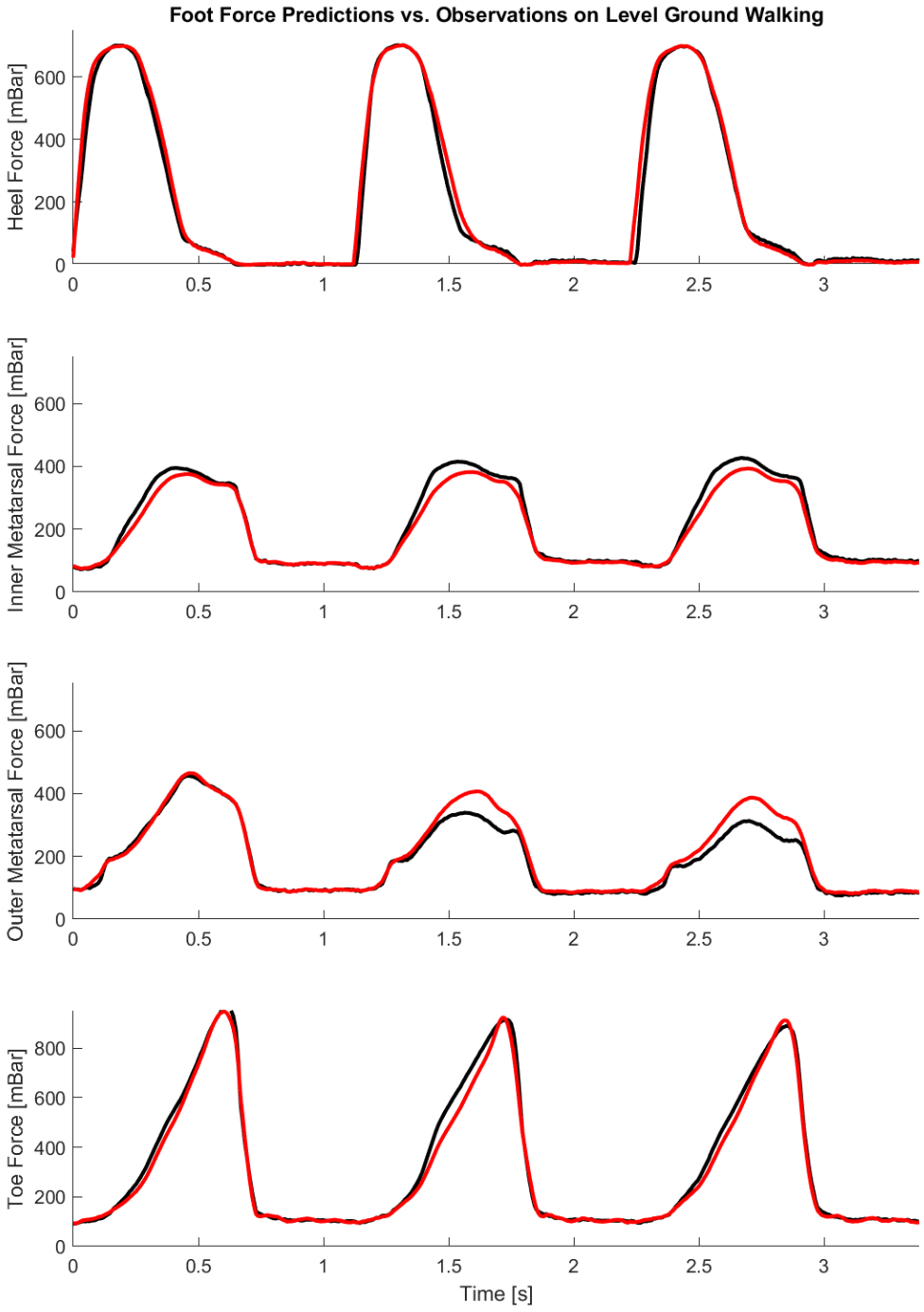

Figure 5.15: Red: Foot force prediction for a single step vs **Black:** foot force observations during same step for level ground walking.

Figure 5.16: Red: Foot force prediction for a single step vs **Blue:** foot force observations during same step shown as a force trajectory across the bottom of the shoe for level ground walking.

5.6 Learning Sloped Interactions

Similar to walking on lever ground, traversing inclines both positive and negative is extremely common in every day walking. Modern powered prosthetics have trouble dealing with sloped walking because common controller types have trouble distinguishing slopes from level ground and therefore produce unsatisfactory control outputs. Some device manufacturers have adjusted for this by adding additional springs into the devices to absorb extra loads but the outputs are still suboptimal. Cyclical interaction primitives hope to improve on the current state of the art by creating distributions around the changes in variable observations given slope conditions such that future states can be accurately predicted. In this section the cyclical interaction primitives, utilizing Phase Projection and von Mises basis functions will be tested on inclined walking in order to test the efficacy at predicting biomechanical features.

For this test a single trial of walking on a treadmill at 3.0mph and 6% grade for five minutes was used. The trial was broken up into two portions such that the first 70% of steps collected during the testing was used for the learning step of Cyclical Interaction Primitives and the final 30% was reserved for the testing step. For this experiment the observed variables that the Cyclical Interaction Primitives are conditioned upon are angular position in 3DOF and angular velocity in the x direction, and the controlled variables of the Cyclical Interaction Primitives are the four foot forces which will be predicted. Results of the testing can be seen in the Table 5.4

Table 5.4: Inclined Walking Prediction Errors

	Immediate Estimation	Prediction
MSE	0.11	0.56
MAPE	54.6	1.15

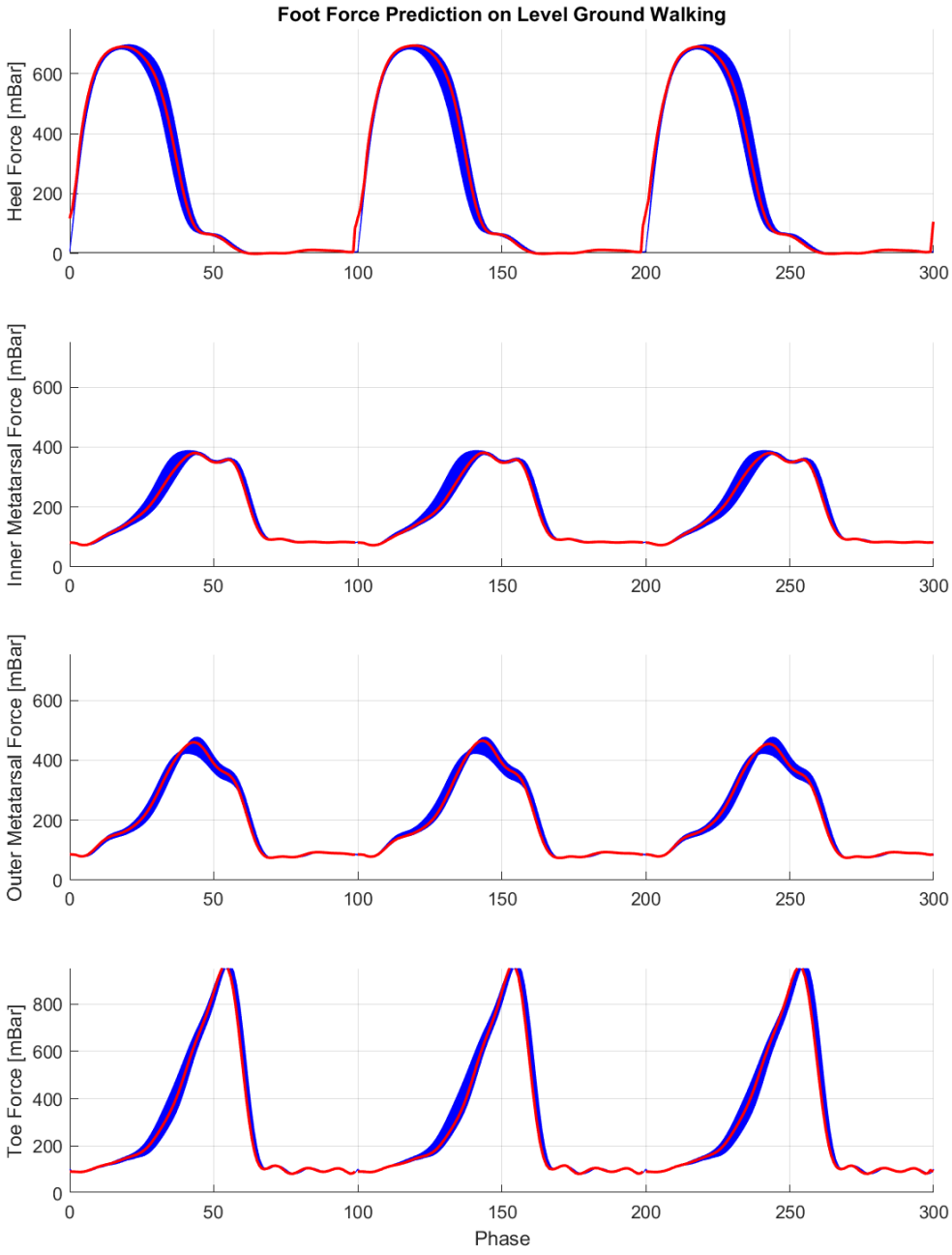

Figure 5.17: Red: Individual foot force predictions for a single step vs **Blue:** foot force standard deviations for inclines.

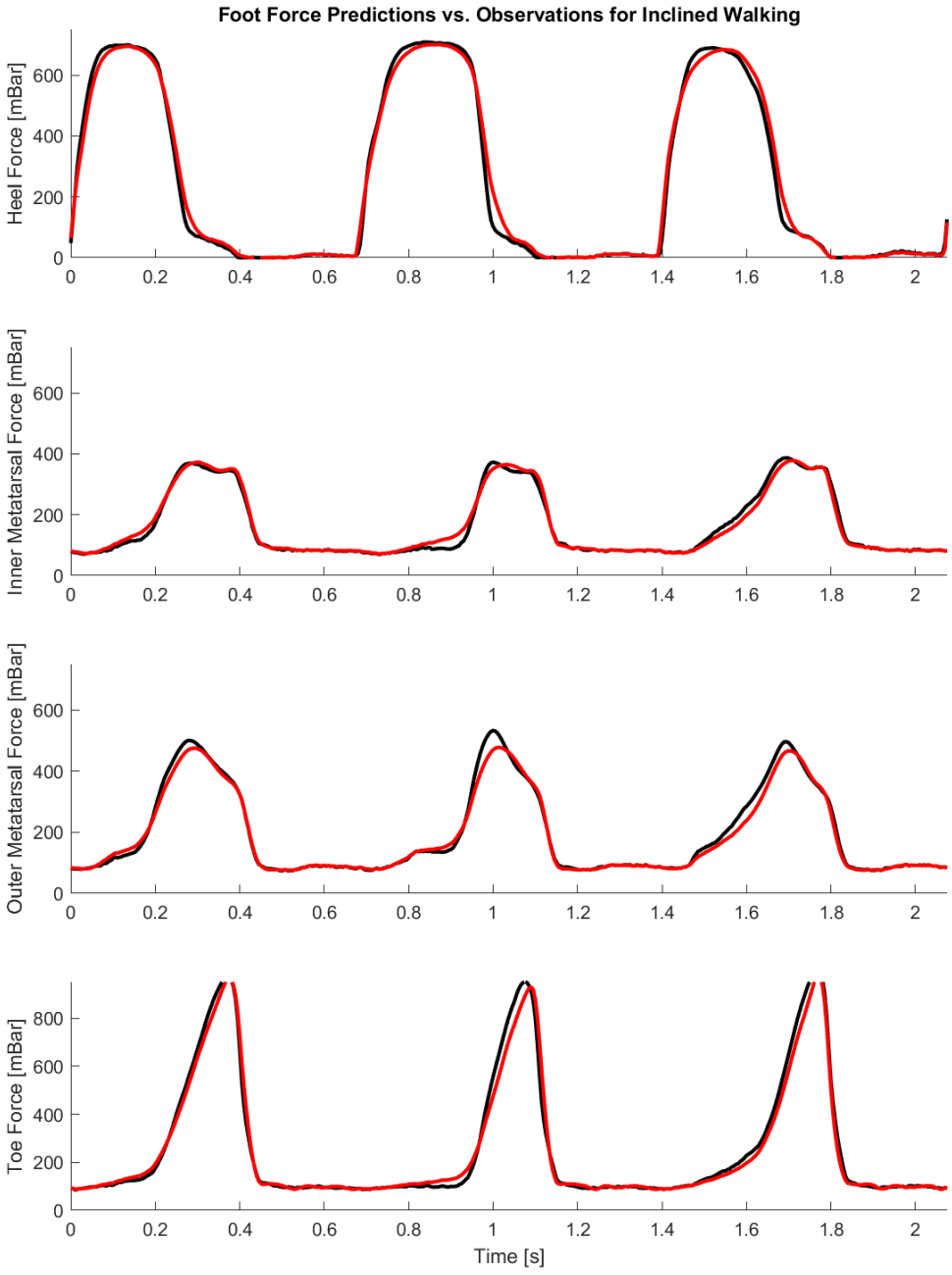

Figure 5.18: Red: Foot force prediction for a single step vs **Black:** foot force observations during same step for inclines.

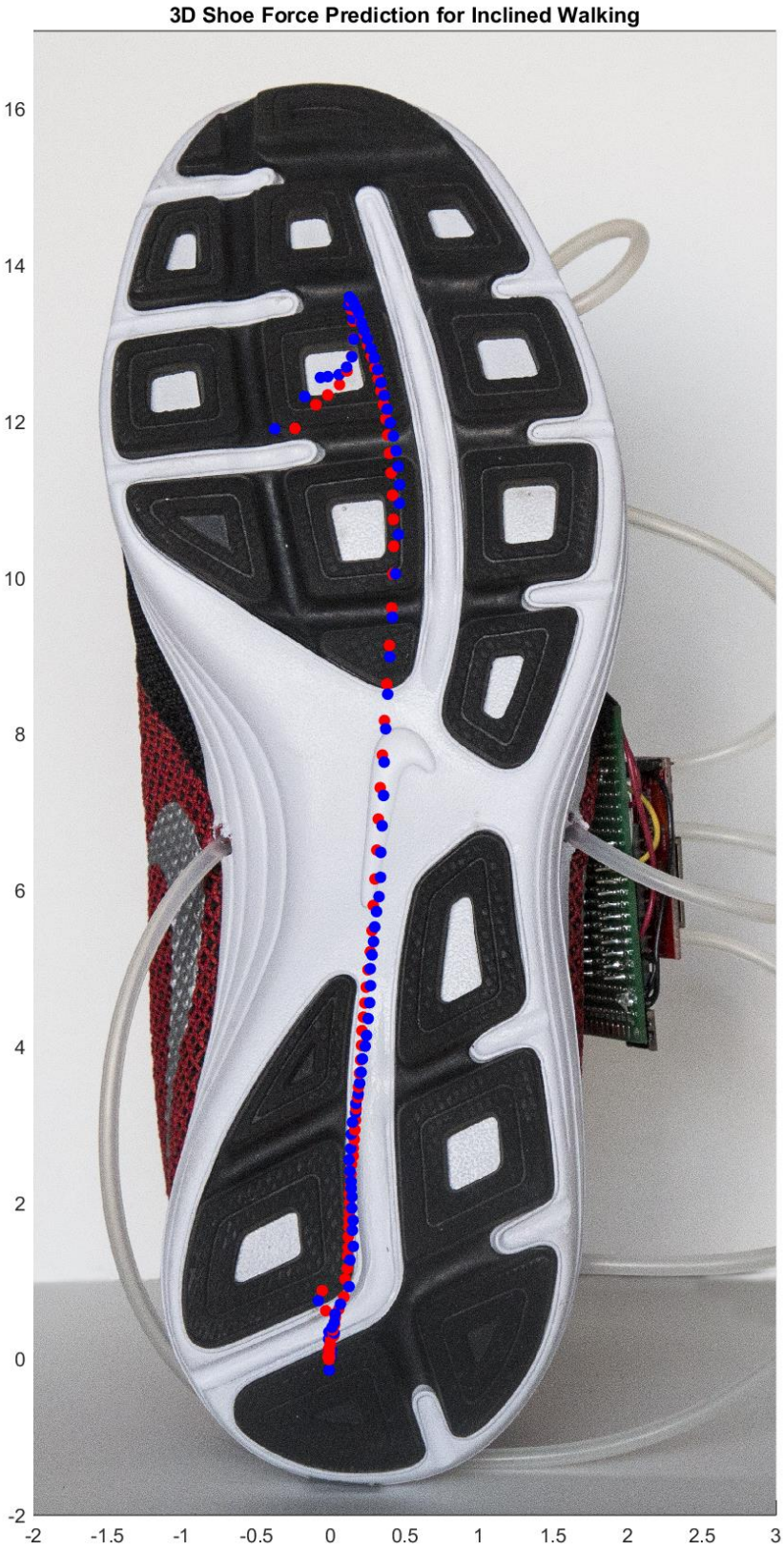

Figure 5.19: Red: Foot force prediction for a single step vs **Blue:** foot force observations during same step shown as a force trajectory across the bottom of the shoe for inclines.

5.7 Learning Stair Climbing Interactions

While level ground and inclines are are fairly easy for a modern prosthetic device to accommodate for, stairs are significantly trickier. A significant amount of time has been put into modifying modern control strategies for powered prosthetics to work with stairs. The best are able to distinguish stairs from normal walking about 99% of the time. If a normal control output for level ground is used while walking up stairs the prosthetic device actuates the ankle far too quickly causing the subject to be pushed backwards. This means that the best robotic prosthetic controllers actively try to kill the human subject about once out of every one hundred steps. This section works to develop an effective biomechanical prediction algorithm based on Cyclical Interaction Primitives, utilizing Phase Projection and von Mises basis functions to predict biomechanical features from distributions of the observed kinematic feature space.

For this test multiple trials of walking up a flight of stairs at a self-selected speed was used. The trials were cut into individual steps and then concatinated to form the full dataset. An additional trial walking up the same flight of stairs was used as the test case. Results of the testing can be seen in the Table 5.4

Table 5.5: Stair Walking Prediction Errors

	Immediate Estimation	Prediction
MSE	0.11	0.56
MAPE	54.6	1.15

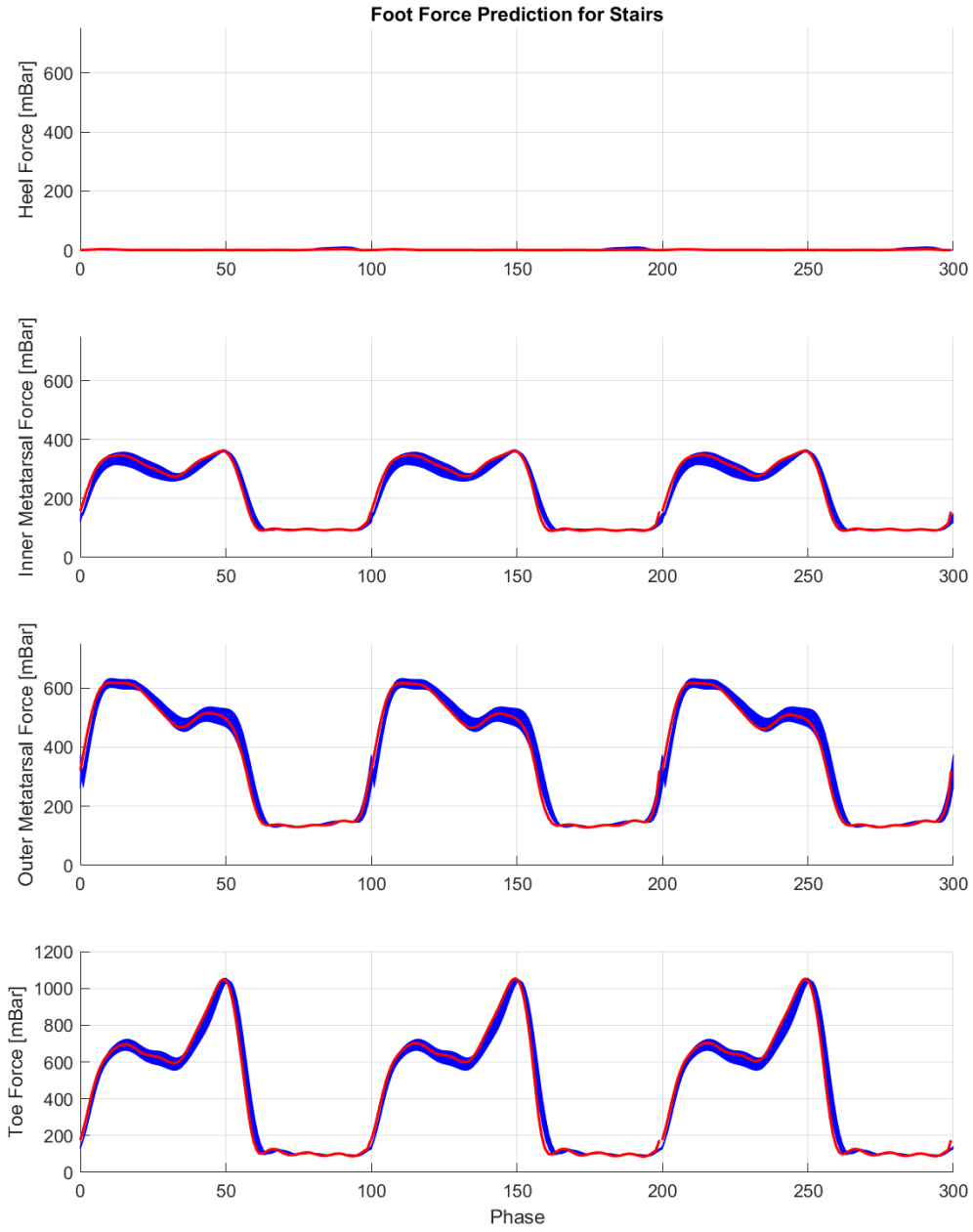

Figure 5.20: Red: Individual foot force predictions for a single step vs **Blue:** foot force standard deviations for stairs.

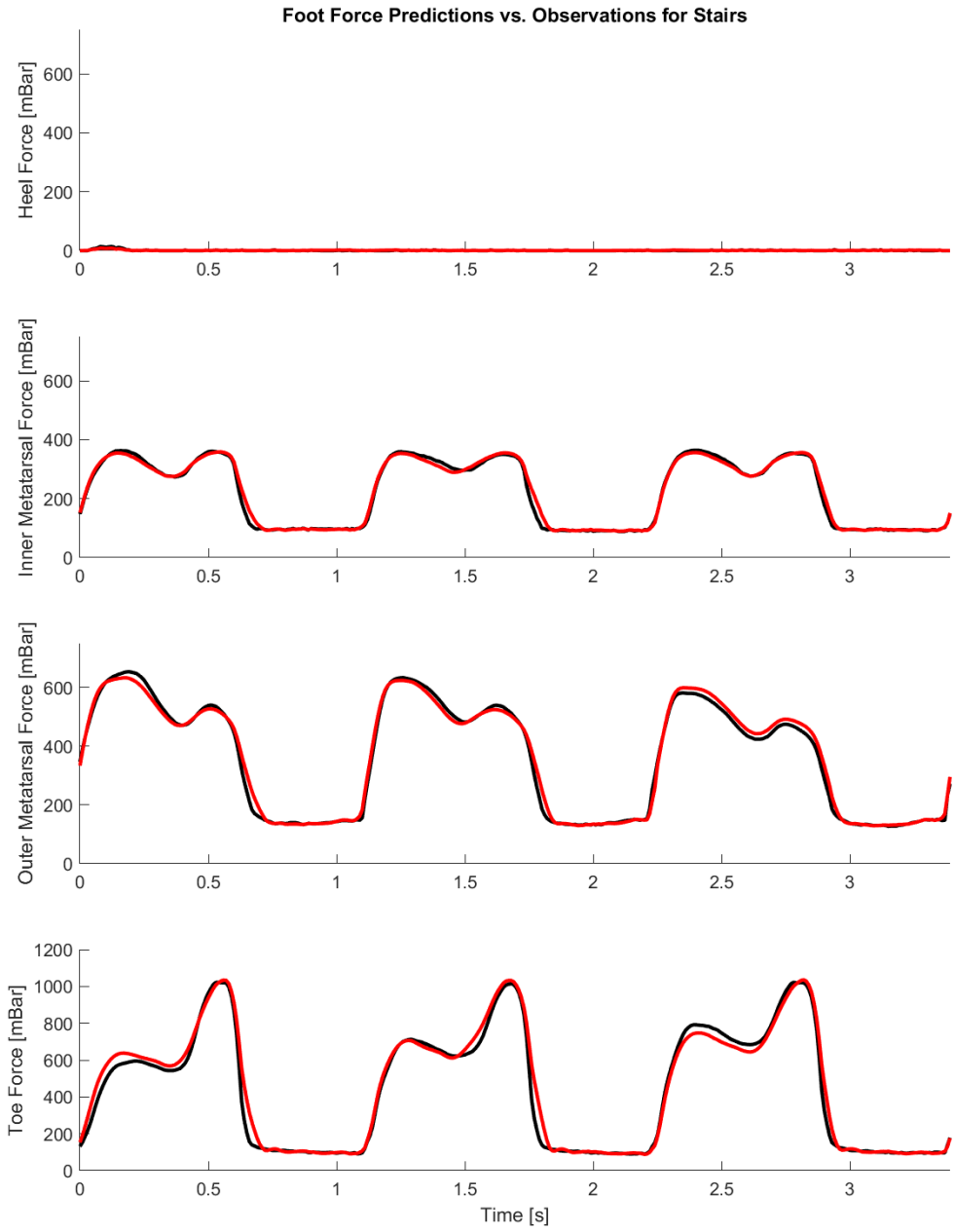

Figure 5.21: Red: Foot force prediction for a single step vs **Black:** foot force observations during same step for stairs.

Figure 5.22: Red: Foot force prediction for a single step vs **Blue:** foot force observations during same step shown as a force trajectory across the bottom of the shoe for stairs.

Chapter 6

CONCLUSION AND FUTURE WORK

6.1 Conclusion

In Conclusion the introduced cyclical interaction primitives are very efficient at generating predictions in real-time of biomechanical features inherent in a humans gait. It supplies excellent estimation during the current time step and is able to predict future states is phase reasonable well as well. Best of all the algorithm is able to run in real-time on the actual devices. Additionally it is important to note that the demonstrations needed to get good results is less than 100 demonstrations.

6.2 Future Work

This Dissertation is the first step towards the larger goal of incorporating the biomechanical well-being of the human user into the robot control and decision making process, entitled Preventative Robotics. In contrast to rehabilitation which seeks to help an individual recover after an injury, Preventative Robotics seeks to reduce the liability of using a prosthetic device by constantly evaluating the gait characteristics of the human user and directing the robotic prosthetic in a way that pro-actively limits the risks of injuries and musculoskeletal disorders. To accomplish this goal there two areas which need further research and study: (1) human state estimation and biomechanical prediction (2) symbiotic control algorithms.

Moreover, it is a goal to transition this research onto a prosthetic ankle. The ankle which will be used is the Ruggidized Odyssey, created by SpringActive Inc., shown in Figure 6.1. The Odyssey ankle comes equipped with custom titanium tension

springs in parallel with a high-power motor and controller. Setting the spring and motor in parallel allows the spring to store energy efficiently while using the motor to add or subtract energy from the gait. The ankle will be controlled using novel micro-controllers and sensors which will facilitate real-time applications.

Figure 6.1: SpringActive inc. Odyssey Robotic Ankle.

6.2.1 Human State Estimation and Biomechanical Prediction

The key question, a question I find incredibly compelling, is how does a humans' intentions, kinematics, and kinetics change in response to robot actions. All research in the field of prosthetics control focuses on an optimal control strategy for a robotic

prosthetic in regard to a human. More important to a humans welfare is what effect that control strategy will have on not just their ability to walk but on their body in general. Any action executed by a prosthetic will have an impact on the state of the human user and will effect not only the immediate kinetics and kinematics of the human but also the response the elicited for the human. The main objective here is to create a feature rich, dynamic representation of the mutual dependencies in a strongly coupled human-robot interaction scenario. This main objective can be broken up into the three subtasks: (1a) biomechanical data augmentation, (1b) predictive modeling of human-robot interaction dynamics, (1c) efficient multi-modal state representation.

Biomechanical Data Augmentation

This area covers this dissertation. To truly understand the interaction happening in the human-robot system both prediction and estimation of internal biomechanical kinematics and kinetics are required. Since truly *in vivo* measurements of joint movements and loads require invasive surgery, the internal variable must be calculated based on other human body parameters. Modern techniques use inverse dynamics on observable variables such as EMG, motion capture data, and force plates to calculate analytically the corresponding non-observable internal variables. However, this is both too costly and too computationally expensive to run in real-time. Therefore instead of using a simulation framework to get analytical solutions, we will utilize the predictive models of Cyclical Interaction Primitives to estimate these internal variables with learned distributions. Internal variable estimation is pivotal to learning the human-robot interaction dynamics.

Predictive Modeling of Human-Robot Interaction Dynamics

A human-robot system that is as tightly coupled as a robotic prosthetic must be thought of as a symbiotic system. Each system effects the other in innumerable ways. The goal is to use a low-dimensional space in order to learn and relate the effects properly such that efficient and safe control can be enacted. Again, instead to trying to develop analytical solutions to this problem, which would be far too computationally expensive to be a reasonable solution, the information and relationships will be extracted from data of real world interactions with a robot prosthetic. The learned model will represent how the actions of the human and robotic prosthetic are mutually affecting and influencing each others high dimensional states. A learned model will provide predictions of future actions of human and robot given current states while maintaining an estimation of the uncertainty underlying these predictions. The most important work here is to create a low-dimensional coupling of the two systems with a projection into a high-dimensional space, which will allow for the efficient modeling of the symbiotic dynamics while employing the high-dimensional space to analyze the ramifications of the pairing.

Efficient Multimodal State Representation

Since these tasks must run in real-time it is important that the models are efficient at storing and utilizing data. Most traditional machine learning approaches do not have significant real-time requirements and those that do mostly make up for it with increased computational power or hardware optimization. Prosthetic devices though bring along with them the additional challenges of having to carry both power and computer on a human body at all times. It is therefore important to develop multimodal models which are effective under these harsh conditions. The strategy incor-

porated will be to use a newly developed method by Joe Campbell in Campbell and Amor (2018). This method utilizes ensemble Kalman filters to reduce the computational dimensionality of the interaction space while enabling more efficient processing of multimodal data. This method is about 50x faster than traditional Interaction Primitives, is more accurate, and more robust. Since it is dealing with multimodal data it also add additional usefulness to Interaction Primitives in its ability to handle multiple different basis function types at once, something traditional Interaction Primitives is incapable of.

6.2.2 Symbiotic Control Algorithms

In the first section a model is produced from collected human-robot interaction data that is able to anticipate the state of both the human and robotic prosthetic and infer the complex relationship between them. This section will utilize this complex model in order to generate optimal control strategies for the prosthetic device. By utilizing the predictive power of the generated model the action space of the prosthetic can be examined to determine the action which minimizes risks to the musculoskeletal system. This goal will also be divided into three distinct tasks: (2a) symbiotic model predictive control, (2b) continuous activity switching via mixtures of symbiotic controllers, (2c) human-machine co-adaptation.

Symbiotic Model Predictive Controller

In order to generate optimal controls outputs given the human-robot state a model predictive controller will be used. A model predictive control acts by minimizing a given cost function over a control horizon given a predicted state. In this case the predicted state will be supplied by the state estimation solution from the Section 6.2.1. In contrast to traditional prediction solutions, this prediction solution will contain

information about the joint symbiotic human-robot relationship. Therefore the model predictive controller will jointly optimize the control signal with respect to its effect on both the robotic prosthetic and the human user. Given state observations from the human user and the intended robot actions, predictions can then also be made regarding the future state of the human movement and impending biomechanical implications. By incorporating the biomechanical implications into the symbiotic model predictive controller, the robot is able to optimize the robot constants, such that control schemes are chosen that elect healthy behavior from the user. The cost function is crucial to the success of this step and different cost function will have to be tested and analyzed for their efficacy on the human biomechanical system and risk of injury.

Continuous Activity Switching via Mixtures of Symbiotic Controllers

It is understood that the symbiotic interactions between human user and robotic prosthetic will encompass a variety of tasks and situations. Learning a single, highly complex model which includes the entire space of possible actions and interactions will likely not function well, as it must be generalizable to all possible scenarios. Instead, a modular architecture for combining a library of models will be used. Individual model and controller schemes will first be trained and designed for specific tasks or situations. Subsequently, individual models are then integrated together via a mixture-of-experts model, which is able to select and combine different model and controllers together through a learned model. As a human user traverses and interacts with the environment accompanied by a robotic prosthetic, the mixture-of-experts model is able to recognize tasks and situations in order to blend a weighted sum of individual controller outputs to perfectly handle the situation.

Human-Machine Co-Adaptation

Each human user will bring with them a new set of biomechanical features and challenges. It is for this reason that human prosthetics users must return periodically to a Prosthetist in order to have their device recalibrate for changes in: the device, gait characteristics, or body shape. A Prosthetist does this through expert observations and feedback from the user. While Prosthetists are trained in traditional methods, modern powered prosthetics have proven a challenge for properly tuning. There are simply to many parameters Prothetists are unfamiliar with in the robotic tuning process for it to be effective. To combat this, the model will incorporate an auto-calibration procedure, that adapts the control parameters to changes in the coupled human-robot system. This adaptation will be framed as a policy search problem under which the cost function is continuously updated in a search process. Of particular interest is finding and quantifying specific features that emerge as a result of the symbiotic dynamical system.

Ackermann, M. and A. J. Van den Bogert, "Optimality principles for model-based prediction of human gait", Journal of biomechanics **43**, 6, 1055–1060 (2010).

Agrawal, V., R. Gailey, C. OToole, I. Gaunaurd and A. Finnieston, "Influence of gait training and prosthetic foot category on external work symmetry during unilateral transtibial amputee gait", Prosthetics and orthotics international **37**, 5, 396–403 (2013).

Amor, H. B., G. Neumann, S. Kamthe, O. Kroemer and J. Peters, "Interaction primitives for human-robot cooperation tasks", in "Robotics and Automation (ICRA), 2014 IEEE International Conference on", pp. 2831–2837 (IEEE, 2014).

Anderson, F. C. and M. G. Pandy, "Dynamic optimization of human walking", Journal of biomechanical engineering **123**, 5, 381–390 (2001).

Burgess-Limerick, R., B. Abernethy and R. J. Neal, "Relative phase quantifies interjoint coordination", Journal of biomechanics **26**, 1, 91–94 (1993).

Campbell, J. and H. B. Amor, "Bayesian interaction primitives: A slam approach to human-robot interaction", in "Proceedings of the 1st Annual Conference on Robot Learning", edited by S. Levine, V. Vanhoucke and K. Goldberg, vol. 78 of *Proceedings of Machine Learning Research*, p. 379387 (PMLR, 2017), URL `http://proceedings.mlr.press/v78/campbell17a.html`.

Campbell, J. and H. B. Amor, "Multimodal inference with ensemble kalman filters for bayesian interaction primitives", in "In Preparation", (2018).

Collins, S. H. and A. D. Kuo, "Recycling energy to restore impaired ankle function during human walking", PLoS one **5**, 2, e9307 (2010).

Farrokhi, S., B. Mazzone, A. Yoder, K. Grant and M. Wyatt, "A narrative review of the prevalence and risk factors associated with development of knee osteoarthritis after traumatic unilateral lower limb amputation", Military medicine **181**, suppl_4, 38–44 (2016).

Holgate, M. A., T. G. Sugar and A. W. Bohler, "A novel control algorithm for wearable robotics using phase plane invariants", in "Robotics and Automation, 2009. ICRA'09. IEEE International Conference on", pp. 3845–3850 (IEEE, 2009).

Hussein, A., M. M. Gaber, E. Elyan and C. Jayne, "Imitation learning: A survey of learning methods", ACM Computing Surveys (CSUR) **50**, 2, 21 (2017).

Ijspeert, A. J., "Biorobotics: Using robots to emulate and investigate agile locomotion", science **346**, 6206, 196–203 (2014).

Lee, D., C. Ott and Y. Nakamura, "Mimetic communication model with compliant physical contact in humanhumanoid interaction", The International Journal of Robotics Research **29**, 13, 1684–1704 (2010).

Lin, Y.-C., J. P. Walter and M. G. Pandy, "Predictive simulations of neuromuscular coordination and joint-contact loading in human gait", Annals of biomedical engineering pp. 1–12 (2018).

Lloyd, C. H., S. J. Stanhope, I. S. Davis and T. D. Royer, "Strength asymmetry and osteoarthritis risk factors in unilateral trans-tibial, amputee gait", Gait & posture **32**, 3, 296–300 (2010).

Maeda, G., M. Ewerton, R. Lioutikov, H. B. Amor, J. Peters and G. Neumann, "Learning interaction for collaborative tasks with probabilistic movement primitives", in "Humanoid Robots (Humanoids), 2014 14th IEEE-RAS International Conference on", pp. 527–534 (IEEE, 2014).

Mattes, S. J., P. E. Martin and T. D. Royer, "Walking symmetry and energy cost in persons with unilateral transtibial amputations: matching prosthetic and intact limb inertial properties", Archives of physical medicine and rehabilitation **81**, 5, 561–568 (2000).

McNealy, L. L. and S. A. Gard, "Effect of prosthetic ankle units on the gait of persons with bilateral trans- femoral amputations", Prosthetics and orthotics international **32**, 1, 111–126 (2008).

Meltzoff, A. N. and M. K. Moore, "Explaining facial imitation: A theoretical model", Early development & parenting **6**, 3-4, 179 (1997).

Meyer, A. J., I. Eskinazi, J. N. Jackson, A. V. Rao, C. Patten and B. J. Fregly, "Muscle synergies facilitate computational prediction of subject-specific walking motions", Frontiers in bioengineering and biotechnology **4**, 77 (2016).

Morgenroth, D. C., A. C. Gellhorn and P. Suri, "Osteoarthritis in the disabled population: a mechanical perspective", PM&R **4**, 5, S20–S27 (2012).

Nandy, A. and P. Chakraborty, "A study on human gait dynamics: modeling and simulations on opensim platform", Multimedia Tools and Applications **76**, 20, 21365–21400 (2017).

Paraschos, A., C. Daniel, J. R. Peters and G. Neumann, "Probabilistic movement primitives", in "Advances in neural information processing systems", pp. 2616–2624 (2013).

Rao, R., "A bayesian model of imitation in infants and robots", Imitation and Social Learning in Robots, Humans, and Animals: Behavioural, Social and Communicative Dimensions (2005).

Royer, T. and M. Koenig, "Joint loading and bone mineral density in persons with unilateral, trans-tibial amputation", Clinical Biomechanics **20**, 10, 1119–1125 (2005).

Sakoe, H. and S. Chiba, "Dynamic programming algorithm optimization for spoken word recognition", IEEE transactions on acoustics, speech, and signal processing **26**, 1, 43–49 (1978).

Sanderson, D. J. and P. E. Martin, "Lower extremity kinematic and kinetic adaptations in unilateral below-knee amputees during walking", Gait & posture **6**, 2, 126–136 (1997).

Schaal, S., "Is imitation learning the route to humanoid robots?", Trends in cognitive sciences **3**, 6, 233–242 (1999).

Smeesters, C., W. C. Hayes and T. A. McMahon, "The threshold trip duration for which recovery is no longer possible is associated with strength and reaction time", Journal of Biomechanics **34**, 5, 589–595 (2001).

Sugar, T. G., A. Bates, M. Holgate, J. Kerestes, M. Mignolet, P. New, R. K. Ramachandran, S. Redkar and C. Wheeler, "Limit cycles to enhance human performance based on phase oscillators", Journal of Mechanisms and Robotics **7**, 1, 011001 (2015).

Svoboda, Z., M. Janura, L. Cabell and M. Elfmark, "Variability of kinetic variables during gait in unilateral transtibial amputees", Prosthetics and Orthotics International **36**, 2, 225–230 (2012).

van Dijk, W. and H. Van der Kooij, "Xped2: A passive exoskeleton with artificial tendons", IEEE robotics & automation magazine **21**, 4, 56–61 (2014).

Winter, D. A. and S. E. Sienko, "Biomechanics of below-knee amputee gait", Journal of biomechanics **21**, 5, 361–367 (1988).

Young, A. J., J. Foss, H. Gannon and D. P. Ferris, "Influence of power delivery timing on the energetics and biomechanics of humans wearing a hip exoskeleton", Frontiers in bioengineering and biotechnology **5**, 4 (2017).

Zhang, J., P. Fiers, K. A. Witte, R. W. Jackson, K. L. Poggensee, C. G. Atkeson and S. H. Collins, "Human-in-the-loop optimization of exoskeleton assistance during walking", Science **356**, 6344, 1280–1284 (2017).